Parametrizing tyre wear using a brush tyre model

Henry Salminen
Royal Institute of Technology
Stockholm, Sweden

December 15, 2014

Acknowledgements

I would like to thank my master thesis supervisor Mohammad Mehdi Davari and examiner Jenny Jerrelind for their support and feedback during the course of the thesis. Special thanks goes to my girlfriend Mikaela Pålsson, who has been of invaluable moral support.

Henry Salminen, Stockholm, 2014

Abstract

Studying rubber wear is important because it can save money, minimize health and environmental issues related to the particles generated from tyre wear and reduce fuel consumption. The wear of rubber is considered to be the result of energy dissipation due to friction. There are many models that describe the dynamical behaviour of vehicles and tyre, but less effort has been dedicated to consider the tyre wear in these models.

The purpose of the thesis was to create an easy to understand and trend-accurate tyre wear model for implementation in a complete car model. The tyre wear in the thesis is determined to be the amount of rubber volume loss due to sliding per unit length that the tyre travels. A literature study was performed with the objective of gaining knowledge of tyre models and the affecting parameters of tyre wear. The most important parameters in determining tyre wear were identified as the forward velocity, side-slip angle, longitudinal slip, vertical load, and tyre inflation pressure. The wear was chosen to be calculated with Archards wear law for these parameters both separately and combined in pairs in order to obtain a deeper understanding of the wear.

The results show that wear is increasing exponentially for the forward velocity. Tyre wear decreases linearly as tyre inflation pressure (vertical bristle stiffness) increases. The vertical load, longitudinal slip and side-slip angle yielded exponentially increasing wear. The most influential parameters affecting the tyre wear were the longitudinal slip and side-slip angle, these yielded wear rates up to 10^7 higher compared with the reference case.

The developed tyre wear model is a good base for future work. More measurement data are needed in order to validate the model. For future work it is also recommended to implement camber angle and temperature dependency in order to study these two important parameters influence on tyre wear.

Nomenclature

Abbreviations

Notation	Description
BM	Brush tyre model
TM	Time model
PM	Parameter model
CM	Complete model
KPI	Kingpin inclination

Greek letters

Notation	Description	Unit
α	Side-slip angle	rad
$\dot{\alpha}$	Rate of change of side-slip angle	rad/s
Ω	Wheel angular velocity	rad/s
λ	Longitudinal slip	$-$
ψ	Normalized slip	$-$
δ_x	Longitudinal bristle deformation	m
δ_y	Lateral bristle deformation	m
δ_z	Vertical bristle deformation	m
ϕ	Bristle angle	rad
Δt	Time increment	s
Γ	Contact area angle	rad
$\ddot{\theta}$	Wheel acceleration	rad/s^2
$\dot{\theta}$	Wheel speed	rad/s
θ	Wheel position	rad

Roman letters

Notation	Description	Unit
F_x	Longitudinal force	N
F_y	Lateral force	N
F_z	Vertical force	N
F_{ze}	Steady state value of the vertical force	N
F_s	Suspension force	N
f_x	Longitudinal force acting on bristle	N
f_y	Lateral force acting on bristle	N
f_z	Vertical force acting on bristle	N
$\bar{F}$	Force vector	N
M_x	Overturning torque	Nm
M_y	Wheel torque	Nm
M_z	Aligning torque	Nm
v_x	Longitudinal velocity of wheel center	m/s
v_y	Lateral velocity of wheel center	m/s
v_z	Vertical velocity of wheel center	m/s
$\bar{v}$	Velocity vector of wheel center	m/s
v_c	Circumferential velocity	m/s
v_{sx}	Longitudinal slip velocity	m/s
v_{sy}	Lateral slip velocity	m/s
$\bar{v_s}$	Slip velocity vector	m/s
q_{zx}	Vertical pressure distribution per unit length in the contact area	N/m^3
x	Longitudinal direction	–
y	Lateral direction	–
z	Vertical direction	–
$\ddot{z}_t$	Vertical acceleration of the tyre	m/s^2
$\dot{z}_t$	Vertical velocity of the tyre	m/s
z_t	Vertical position of the tyre	m
z_{te}	Vertical position of the tyre at steady state	m
$\ddot{z}_c$	Vertical acceleration of the car	m/s^2
$\dot{z}_c$	Vertical velocity of the car	m/s
z_c	Vertical position of the car	m
c_{px}	Longitudinal bristle stiffness per unit length	N/m^2
c_{py}	Lateral bristle stiffness per unit length	N/m^2
c_{pz}	Vertical bristle stiffness per unit length	N/m^2
$c_{pz,d}$	Default vertical bristle stiffness per unit length	N/m^2
d_{px}	Longitudinal bristle damping per unit length	Ns/m^2
d_{py}	Lateral bristle damping per unit length	Ns/m^2
d_{pz}	Vertical bristle damping per unit length	Ns/m^2
p_t	Normalized tyre inflation pressure	–
f_{z0}	Nominal tyre load	N
n	Number of bristles	–
sa	Segment angle	rad
m_c	Quarter car mass (sprung mass)	kg
m_t	Tyre mass (unsprung mass)	kg
k	Strut spring stiffness coefficient	N/m
d	Strut damping coefficient	Ns/m^2

Roman letters

Notation	Description	Unit
$w_x(i)$	Longitudinal work performed by the $i:th$ bristle	J
$w_y(i)$	Lateral work performed by the $i:th$ bristle	J
$w_z(i)$	Vertical work performed by the $i:th$ bristle	J
W_x	Sum of longitudinal work	J
W_y	Sum of lateral work	J
W_z	Sum of vertical work	J
Q	Archard's wear quantity	m^3
Q_0	Reference wear	mm^3
Q_c	Current wear	mm^3
Q_n	Normalized wear	-
s	Sliding distance	m
H	Hardness of the worn material	N/m^2
K	Dimensionless specific wear factor of adhesion and abrasion	$-$
F_n	Normal load	N
J	Inertia of the wheel	m^4
M_e	Engine torque	Nm

Contents

Chapter 1

Introduction

1.1 Motivation and background

Since the invention and implementation of the pneumatic tyre some 70 years ago, significant progress has been made both with regards to cars and tyres. The cars of today are significantly safer and at the same time more comfortable compared with only 20 years ago. The key factors for this are the development of various electronic control systems such as air bags and ABS brakes and the advancements of the computers, which now play an intricate part in almost every newly produced car. The advancement of computers have also granted car manufacturers the ability to construct detailed and accurate simulations of cars and driving conditions. This is a major benefit, it allows car manufacturers to alter, improve and find flaws in the design and construction before production starts, thereby saving both money and time, which in turn will most likely lower the purchase cost for the consumer.

Figure 1.1 illustrates how different parameters affect the environment, handling safety and comfort of a car. A large portion of the tyre wear and fuel consumption is contributed by the tyres, as can be seen in Figure 1.1. By improving the tyre characteristics the environmental impact could be significantly lowered.

Over the last 15 years the production of cars has increased from roughly 40 million to an estimated 65 million (2013), [1]. The production is also expected to grow, since China and India are demanding even more cars for their growing population. It becomes apparent that if only a small increase in the tyre life cycle and a small reduction in rolling resistance can be achieved on every new tyre for every new car, then a large amount of fuel can be saved. Tyre wear is also costly for consumers that need to buy new tyres and for the environment since it generates large amounts of waste as well as particle emission affecting both the environment and organic life. It is therefore relevant to determine how tyre wear can be minimized and what which parameters affect wear.

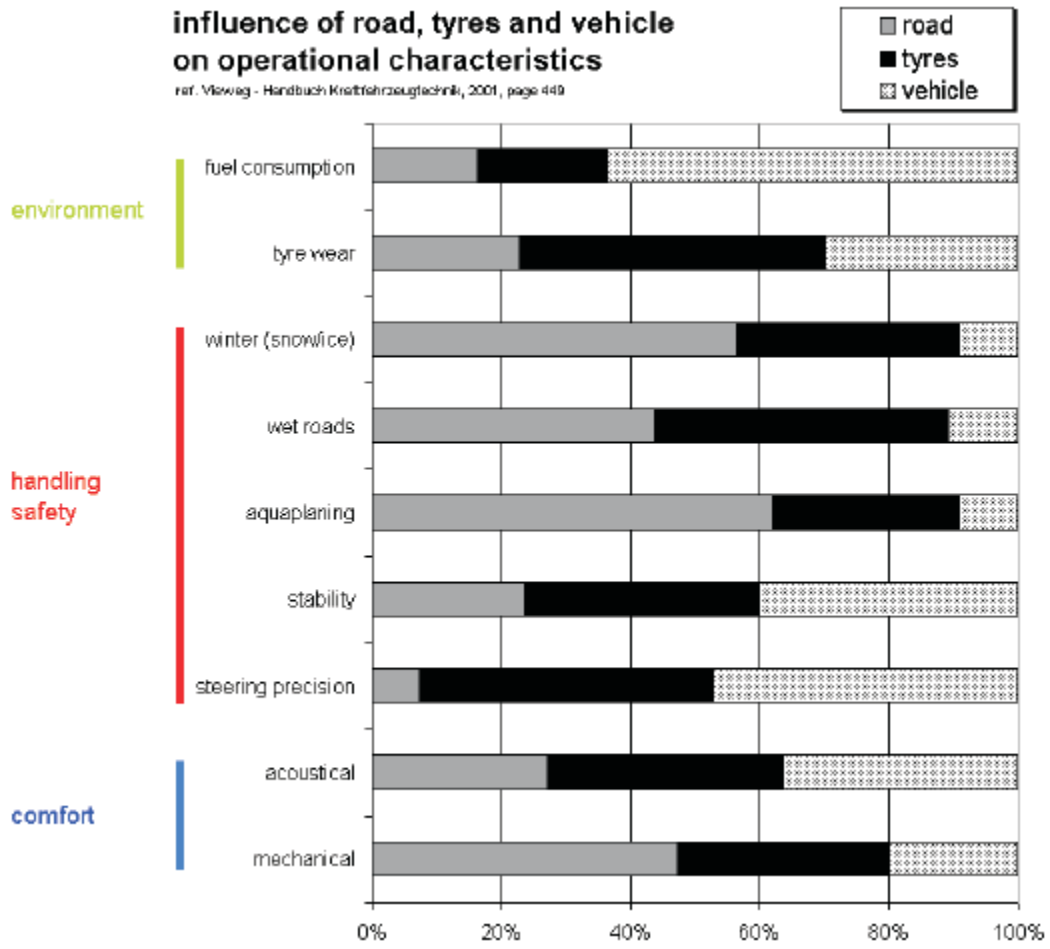

Figure 1.1: From left to right, the influence of road, tyres and car on environment, safety and comfort, [2].

1.2 Aim and scope

The main purpose of the thesis was to create a tyre wear model which accurately illustrates wear trends for chosen input parameters. The model will then be used in simulations of new passenger car chassis concepts to reveal the best dynamic situation of the wheel-chassis unit to reduce the wear of the tyre.

The work was divided into different work packages.

- A literature survey to gain a better understanding of tyres, tyre wear and tyre models. Identifying which model or models to use and under which circumstance they are valid.
- Put together a basic tyre model which could be extended to include relevant car and tyre parameters.
- Choose a wear model and implement it in the tyre model.
- Investigate which parameters have the largest effect on tyre wear and implement them into the model.
- Make different simulations with the developed tyre wear model and analyse the results.

The scope of the thesis was to deliver a working tyre wear model which include input parameters which are relevant to the wear of tyres. The model should be easy to understand and have a physical interpretation so that anyone with some knowledge of both programming and tyre models could understand it.

1.3 Outline of the thesis

The outline of the thesis is as follows.

In Chapter 2 the literature study is presented, it is divided into four parts. The first part describes the basics of the tyre. The second part contains a description of the modern bias radial tyre, definition of the coordinate system, kinematic tyre concepts and tyre settings. The third part contains the causes of tyre wear and finally the forth part covers the tyre and wear models.

In Chapter 3 the desired model properties are defined and an evaluation of the researched models is conducted. The first part of Chapter 3 is dedicated to defining the requirements, application and limitation of the model. In the second part the tyre models of interest are explained and then ranked. The last part deals with choosing a suitable tyre and wear model.

Chapter 4 contains a description of the chosen tyre and wear model and implementation in MATLAB. The interaction between the models is illustrated in a flowchart.

Chapter 5 contains the wear results, illustrated as a function of one and two input parameters along with comments and discussion regarding the results.

Finally, in Chapter 6, conclusion, recommendations and future work.

Chapter 2

Literature study

Before starting with the tyre wear model it is important to first understand the fundamentals of the tyre it self and how it is composed. Starting with the structure of the tyre and then moving on to how it's generally defined in a model, with different sign conventions, angles, velocity vectors, force vector and moments. After that, the different conditions or mechanism of wear are described followed by a list of the different tyre parameters and their affect on the tyre wear. Finally, a brief description of the most common tyre models and wear models.

2.1 The tyre

Tyres provide grip between the road surface and the wheel while acting as a flexible cushion, like an additional spring. Since the tyre is the only connection between the road surface and the car it therefore carries all the load from the car to the road. Consequently, the tyre needs to be able to withstand large forces, not only by the vertical forces from the car itself, but forces generated during cornering, acceleration and braking. These forces will deform the tyre and it will most likely be absorbed in the carcass and tread.

The modern tyre is rather complex as can be seen when studying Figure 2.1. The exact composition of a tyre may vary with different manufacturers, but the general structure is the same. A full explanation of all notations and parts in the tyre from Figure 2.1 follows in Table 2.1.

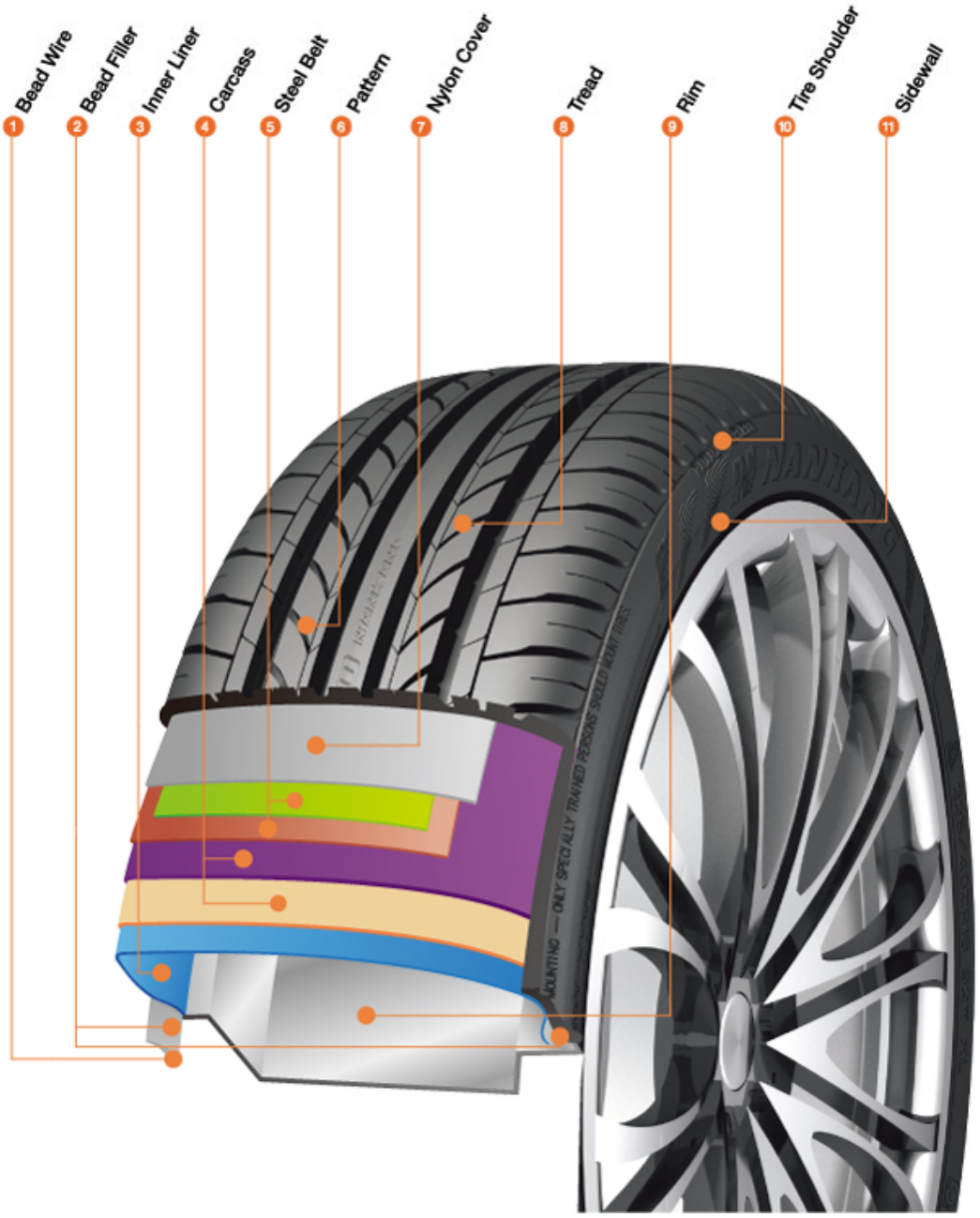

Figure 2.1: Structure of the modern tyre, [3].

Table 2.1: Explanation of notations in Figure 2.1.

Item number	Item name	Description
1	Bead wire	The bead wire is located on both sides of the rim, it circles around the rim several times and its purpose is to hold the tyre on the rim and prevent air from escaping. It is therefore very heavily reinforced so that it creates a tight fit on the rim, this is to ensure that it does not move radially during rotation, which would otherwise lead to air leakage.
2	Bead filler	The bead filler is a thick layer of hard rubber that is meant to keep the bead wire in place and to ensure that the bead wire does not damage other components of the tyre.
3	Inner Liner	The inner liner is the inner part of the tyre, that is in contact with the air that fills the tyre. It is usually quite thin and it's purpose is to seal in the pressurized air. It's rubber compound with low air permeability.
4	Carcass	The carcass is the main body of the tyre. It sustains the inflation pressure and has to be able to withstand shocks and endure heavy loads. There are three major construction approaches, the bias ply, radial ply and bias belted ply, see Figure 2.2. The properties of the tyres with these construction types are explained below.
5	Steel belt	The steel belt in tyres is located above the carcass and underneath the nylon cover. Its purpose is to give the tyre more rigidity which in turn yields a greater durability. There are often more than one layers of steel belts.
6	Pattern	The tread pattern is characterized by the shape of the grooves, lugs, voids and sipes. Grooves run circumferentially around the tyre and are needed to channel water away. Lugs are the portion of the pattern which is in contact with the road surface. Voids are spaces between the lugs which facilitates water removal and gives the lugs leeway to flex. Sipes are cuts, orthogonal to the tyre velocity vector which are designed to channel away from the pattern. The pattern of a tyre tread depends greatly on the designed use of it. For passenger car tyres there are several different patterns, for example rib, asymmetric, block and zigzag. Rib pattern tyres have a patter in the v-like shape. This pattern facilitates water drainage from the tyre, making it ideal for wet conditions. Asymmetric tyres have different patterns on the inside and outside of the centreline of the tread. These patterns are designed usually for high performance cars which get the benefit from the good cornering ability of the inside of the tread and the good water drainage of the outside of the tread. Block pattern tyres are mostly used for winter or all season type tyres. Zigzag patterns are of ideal use during long journeys due to their low rolling resistance, they do however posses poor cornering properties and suffer from a lack of grip in both wet and dry conditions,[4].
7	Nylon cover	The nylon cover is meant to separate the tread and the steel belts and also stabilize the tread.
8	Tread	The tread of a tyre is the part of the tyre that comes in contact with the road surface and the portion of the tyre that is in contact with the road surface at a given time is called the *Contact patch* or *Contact area*. The tread, as mentioned before, contains the pattern of the tyre. The pattern in turn is characterized by the shape of the grooves, lugs, voids and sipes.
9	Rim	The rim is the medium of the tyre where the beads of the rubber tyre interacts with the wheel axis. Tyres are mounted onto the rim by forcing the bead onto the channel formed by the wheel's inner and outer rims.
10	Tyre shoulder	The shoulder is the area between the edge of the tread and the side wall. This area is also the thickest part of the tyre, because this is where the deformation of the tyre usually occurs.
11	Side wall	The side wall of the tyre extends from the leading edge of the rim to the shoulders. The side wall is largely made of rubber but also reinforced with cords of different materials to increase strength and flexibility,[5],[6].

2.2 Tyre construction and terminology

There are three major types of tyres which are called the bias ply tyre, the bias belted tyre and the radial ply tyre. The names refer to how the plies in the carcass are oriented, this can be seen in Figure 2.2. It can be seen that the bias ply tyre does not contain any belts and has its ply oriented in a criss cross pattern. The radial ply tyre includes belts and has its ply oriented, as the name suggests, in radial direction. The belted bias also has belts and has its ply oriented as the bias ply tyre.

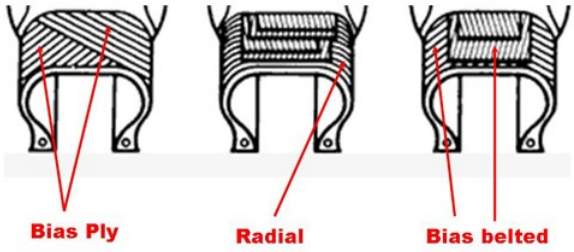

Figure 2.2: The difference in ply orientation for the bias ply, radial ply and bias belted tyre construction types, [7].

2.2.1 Bias ply tyre

The bias ply, also called the cross ply, is a construction of the carcass that uses cords ply cords that extend diagonally from bead to bead, at angles ranging from 30° to 40°. The plies are placed in a criss-cross pattern onto which the tread is then applied. The advantage of this construction technique is that it allows for the carcass and in fact the entire tyre to flex easily, giving the bias ply a smooth ride on rough surfaces. This also yields the major disadvantage of the of the bias ply tyre; high rolling resistance, less control and less grip at high speeds [5].

2.2.2 Bias belted tyre

The bias belted tyre is similar to the bias ply tyre as it also has bias plies. The difference is that stabilizing belts are added which gives the construction roughly the same smooth ride as the bias ply but with a lower rolling resistance [5].

2.2.3 Radial ply tyre

The radial ply tyre is a construction method where the cord plies are arranged in the radial direction of the tyre. The advantage of this construction include longer tread life, better steering control and lower rolling resistance. Disadvantages include a harder ride and lower grip at low speed.

Out of the three construction types the most common used tyre construction for passenger cars is the radial ply tyre which represents 98 % of all tyres in passenger cars [8].

2.2.4 Reference coordinate system and tyre kinematic concepts

The reference coordinate system used in this thesis is defined in Figure 2.3. This largely follows the SAE standard with the longitudinal direction pointing in the wheel heading and the lateral direction pointing perpendicular to the wheel heading and the vertical direction pointing downwards. The positive direction of the forces and torques that can act on a tyre are defined in Figure 2.3

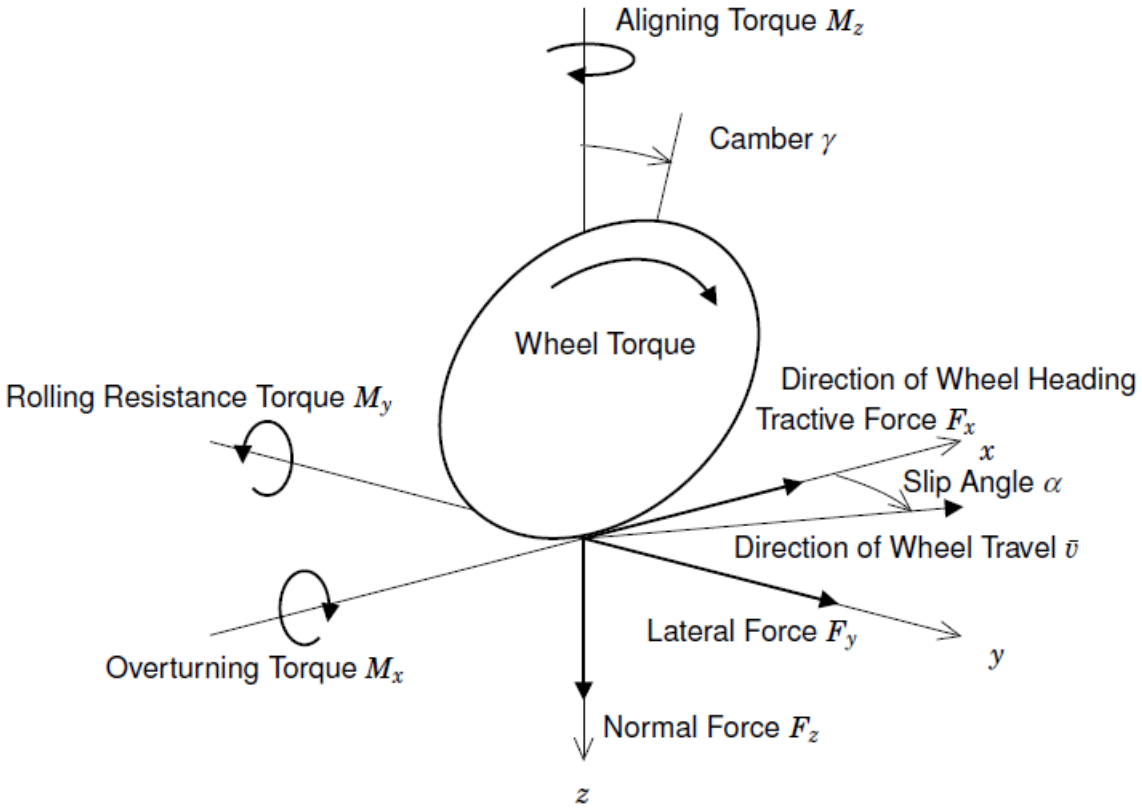

Figure 2.3: Forces and moments acting on a tyre, [9].

The forces acting on the tyre are the tractive force or *longitudinal force* F_x, the *lateral force* F_y and the *normal force* F_z. The moments acting on the tyre are the *overturning torque* M_x, the *wheel torque* M_y and the *aligning torque* M_z. The longitudinal force F_x and the wheel torque M_y is generated when braking or accelerating. The lateral force F_y and overturning torque M_x when cornering. The vertical force F_z is the load of one quarter of the car and the aligning moment is generated as the tyre rolls. However, in this thesis the overturning torque M_x is not considered, as it generally is the result of camber, [10]. The forces are related to the velocities as illustrated in Figure 2.4.

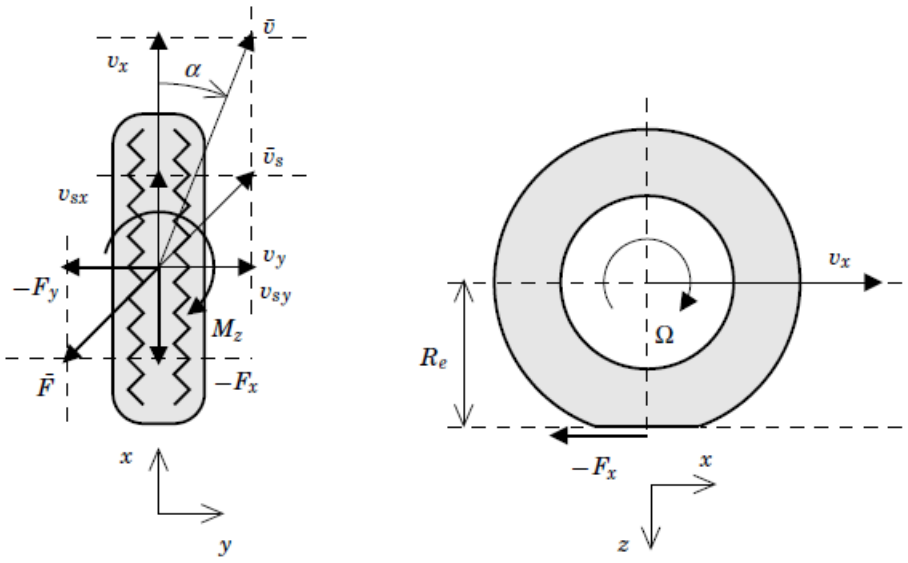

Figure 2.4: Kinematics of an isotropic tyre while braking and cornering, top view (left) and side view (right). [9].

From Figure 2.4 basic tyre kinematic concepts can be defined. The *side-slip angle*, α, is defined as

$$\alpha = \arctan\left(\frac{v_y}{v_x}\right) \tag{2.1}$$

and the *circumferential velocity* as

$$v_c = \Omega \cdot R_e \tag{2.2}$$

where Ω is the *wheel angular velocity* and R_e is the *effective rolling radius*. The relative motion of the tyre in the contact area to the ground is defined as

$$v_{sx} = v_c - v_x \tag{2.3}$$

The slip velocity v_{sx} is normalized with a reference velocity yielding

$$\lambda = \frac{v_c - v_x}{\max(v_x, v_c)} \tag{2.4}$$

which is referred to as *longitudinal slip*. Equation 2.4 can be interpreted as either braking or accelerating. When $v_x > v_c$ the tyre is subject to braking, which in the extreme case $v_c = 0$ m/s yields $\lambda = -1$. If $v_x < v_c$ the tyre is subject acceleration, which in the extreme case $v_x = 0$ m/s yields $\lambda = 1$.

2.2.5 Tyre and suspension structure

The composition of the tyre and suspension is an intricate structure of beams, springs and joints, which is illustrated in Figure 2.5. The purpose of the suspension is mainly to keep the tyre in contact with the road, minimize the rolling motion, add additional ride comfort in combination with the tyres and to absorb road unevenness. And also to ensure that the tyres have contact with the road, thereby enabling the transfer of

forces and moments generated from the engine onto the road surface, for example during braking or cornering, [11].

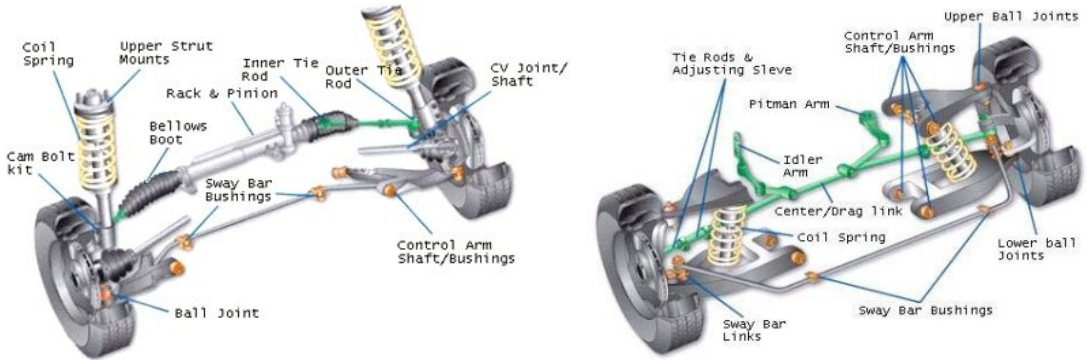

Figure 2.5: Front (left) and rear (right) suspension of a car, [11].

The suspension is designed to absorb shocks by allowing the springs in the shock absorbers to deform and compress and then release. The energy stored in the spring causes it to oscillate with a decreasing amplitude until it finally settles. The decrease in amplitude is achieved by the damper in the shock absorber and also the inner friction in the suspension. The design mitigates the effect of transient behaviour, such as bumps in the road or rapid turns, which would otherwise yield extra loads on the tyre. The suspension arm is attached to a vehicles chassis which supports the wheel hub and allows the suspension to move through its normal range of movement. The bushings are connections between various metal components that allows movement in a smooth and controlled manner without any significant wear, [11].

2.2.6 Wheel and suspension settings

In an ordinary passenger car there are several settings of the wheel and suspensions which affect the wear of a tyre. A stiff suspension for example will increase the loads experienced by the tyre and also decrease ride comfort. However, stiff suspension in combination with a lowered chassis will increase a cars ability to take a corner at a higher speed due the to lessened tendency to pivot and the lower centre of gravity. The main tyre and suspension settings are described below.

Camber

Camber is the angle from the normal of the road surface through the centre of the wheel to the centre line of the wheel, which is illustrated in Figure 2.6. Negative camber occurs when the top of the wheels is pointing towards the centre line of the car, positive camber is the opposite. Camber is mostly used on the front tyres but it is not uncommon to have a slightly negative camber on the rear tyres as well. When a wheel has a camber angle, the interaction between the tyre and road surface causes the wheel to tend to want to roll in a curve, as if it were part of a conical surface, this is called *camber thrust*. The point of having negative camber is that it improves the cornering ability of the car. The reason for this improvement is, while taking a corner the outer tyre is at a more preferable angle relative to the road surface, transmitting the forces through the vertical plane of the tyre rather than through a shear force across it. This creates a larger contact area which increases the grip for the outer tyre. The inner tyre will on the other hand reduce its contact area thus decreasing its grip. The effect that the negative camber has on the outer tyre outweighs the loss of grip from the inner tyre. If on the other hand a set of tyre has positive camber the opposite will occur, meaning that the inner tyre will get an increase in grip whilst the outer tyre will get a decrease in grip due to a narrower contact area. Camber does affect grip when travelling in a straight line in a negative manner, because the contact area is smaller compared to a tyre with zero camber, [12].

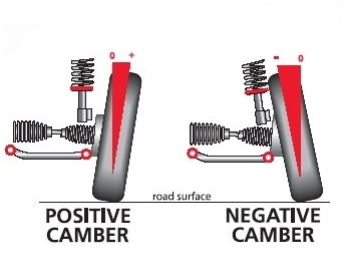

Figure 2.6: Illustration of camber, [13].

Toe

Toe is not easy to notice on a normal passenger cars. It is defined as, observing from above, the symmetric angle that each tyre makes with the longitudinal axis of the car, which is illustrated in Figure 2.7. Positive toe or *toe in* occurs when the tyres point towards the centre line of the car, negative toe or *toe out* is the opposite, [14]. For rear wheel drive cars, having a slight toe in greatly increases straight line stability at the cost of a somewhat unresponsive feel to the steering. Having any sort of toe increases tyre wear since it's basically adds a constant *side-slip angle* on the tyre. However, if a tyre has a camber angle a small degree of toe will cancel or reduce the camber thrust thus reducing the wear and rolling resistance.

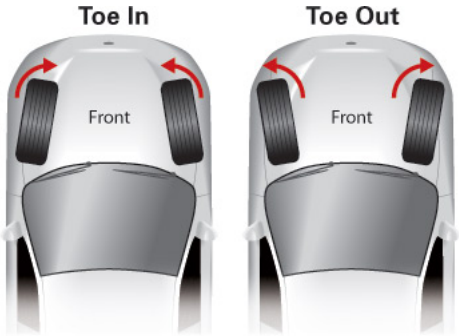

Figure 2.7: Illustration of toe, [15].

Kingpin inclination and caster

Kingpin inclination and Caster are related to each other by the origin of the kingpin axis. Seen from the front, the kingpin inclination angle (KPI) is formed by the angle between the kingpin axis and the centre line of the tyre. Positive KPI is when the top of the kingpin axis is pointing towards the centre line of the car, and negative KPI is when the top pointing away from the centre line. The purpose of the KPI is to ensure the self alignment of the tyres. Together with camber it provides a centre point steering, so called *Ackerman steering*. Its achieved by shortening the steering linkage, thus creating a trapezoid. This makes all tyres corner around a fictive point called the centre of turning, which is illustrated in Figure 2.8. This reduced the side-slip angle which would otherwise be much greater and hence reduces wear [16]. From the side the caster angle is the angle that the kingpin axis makes with the vertical line through the wheel centre. Both KPI and caster are illustrated in Figure 2.8, [17].

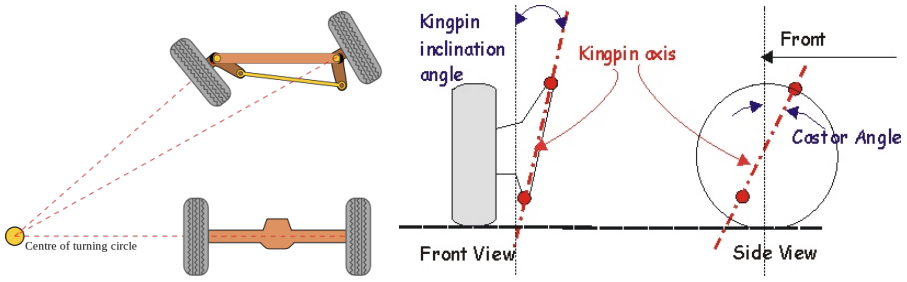

Figure 2.8: Ackermann steering (left) and the definition of KPI and caster(right)

2.3 Rubber wear

The wear of rubber is considered to be the result of energy dissipation due to friction, which can be divided into adhesion and hysteresis. Adhesion occurs when two solid sliding surfaces slide over each other under pressure. Hysteresis occurs during the return to a normal state of a rubber from either compression or expansion. The cause of this is internal friction, [18], [19], [20]. Since rubber is a visco-elastic material the schematic diagram of friction and wear mechanism shown in Figure 2.9 applies to tyres.

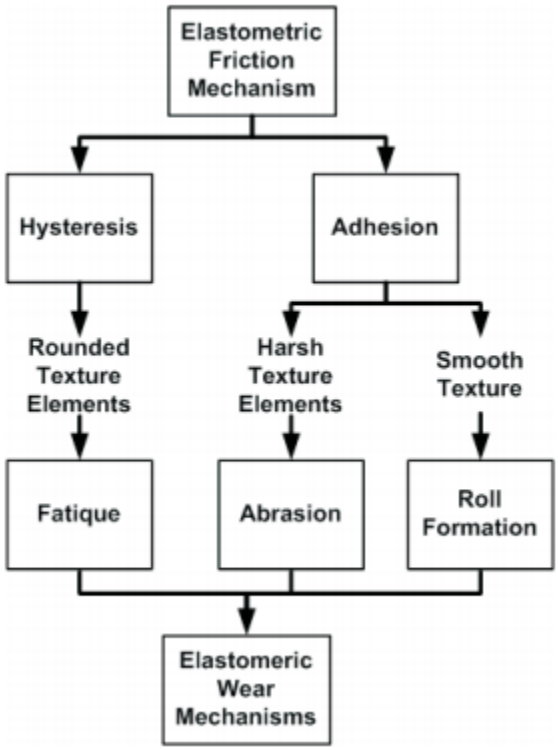

Figure 2.9: Shematic diagram of the friction and wear mechanism in tyres, [18].

2.3.1 Adhesion and abrasive wear

Abrasive wear is a product of adhesion and pressure. The result is a temporary bond between the road and the rubber molecules in the tyre. The bonds are torn apart due to continuing sliding, which results in abrasive wear. The coarseness of the surfaces affects the amount of contact the surfaces have against each other, smoother surfaces have a larger contact area compared to rough surfaces. On rough surfaces such as asphalt the roughness might cause local adhesion peaks, due asperities, resulting in abrasion. Abrasive wear is a function of the texture property, rubber property, vertical load and sliding velocity. The higher the load, the more material will be squeezed between the asperities, increasing the contact area resulting in stronger bonds and therefore higher abrasive wear. Increasing the sliding velocity tears the bonds apart faster leading to a larger abrasive force which increases the abrasive wear, [18].

2.3.2 Hysteresis wear

This type of wear originates from the penetration of the asperities into the tyre, creating high and low deformation areas, which is illustrated in Figure 2.10. The sliding motion of the rubber creates pressure hysteresis in the tyre. This type of wear is relatively mild but it is a continuous process, [18].

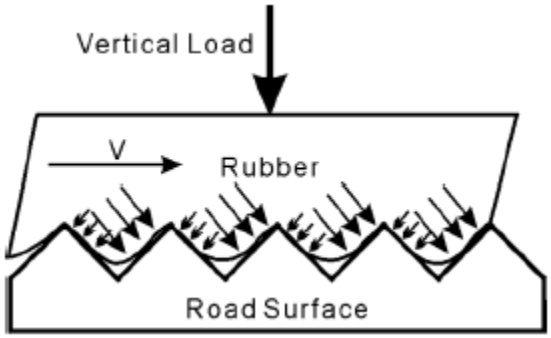

Figure 2.10: Deformation and forces leading to hysteresis wear, [18].

2.3.3 Overall wear

The overall wear is a combination of hysteresis wear and adhesive wear. Considering short test distances the hysteresis wear can be neglected as the adhesive component is much more dominant. However, hysteresis wear can have an effect on longer test cycles due to the behaviour of this type of wear.

The focus in this thesis, modelling the tyre wear, will be put on abrasive wear, which is a sub-category to adhesive wear. This category of wear occurs when elements of the tyre is exceeding the friction force limit and begin to slide.

2.4 Causes of tyre wear

The wear of the tyre is defined as "Damage to a solid surface (generally involving progressive loss of material) caused by the relative motion between that surface and a contacting substance or substances". The wear of tyres is dependant on many parameters these include but are not limited to, [21]:

- Contact geometry
- Length of exposure

- Interacting material surfaces
- Normal force
- Sliding speed
- Environmental conditions
- Material composition and hardness

2.4.1 Contact geometry

The size and shape of the contact surface between the road and the tyre plays a large role in the wear of a tyre. That is also why tyre inflation pressure is of such large importance. The effect of the inflation pressure is displayed in Figure 2.11.

Figure 2.11: Geometry of tyre in the lateral direction for correct, under and over inflation pressures, [22].

Studying Figure 2.11 a conclusion regarding wear can be drawn. For low inflation pressure the tyre wear is concentrated on the shoulders of the tyre and for high inflation pressure its concentrated on the middle of the tyre. High inflation pressure also yields a shorter contact length which also affects the load on the tyre in the contact area, since it must withstand higher pressures, because the same load is distributed over a smaller area. This yields greater deformation of the rubber hence larger wear.

2.4.2 Length of exposure

The longer the tyre is driven the more wear it suffers. Longer exposure leads to higher temperatures leading to higher inflation pressure in the tyre.

2.4.3 Interacting material surfaces

The road surface is never completely flat, meaning the unevenness of the road is causing irregular wear on the tyre surface, this is illustrated in Figure 2.12. The results of the rough road are that parts of the rubber in the tyre want to grip the unevenness of the road causing the fabric to tear causing small cuts. This phenomenon is called abrasive wear.

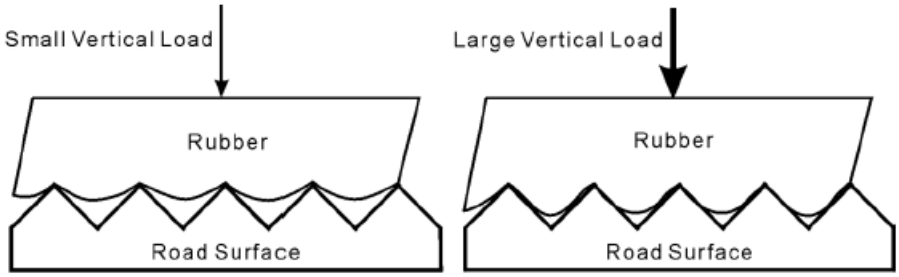

Figure 2.12: Effect of increasing vertical load on tyre rubber, [18].

2.4.4 Normal force

The load acting on the tyre contact surface is a logical cause of wear. Higher loads cause greater deformations and higher strain on the side wall and tread which causes fatigue and therefore wear.

2.4.5 Sliding speed

Sliding causes wear because the wheel angular velocity and the forward velocity of the wheel are unequal. Sliding could also occur in strong wind conditions, where the wind generates a lateral force acting on the tyres. Sliding speed affects wear because, high sliding velocity generates more work, higher work equals more wear.

2.4.6 Environmental conditions

Natural events like heat waves, rainfall, snow and frost all affect the road surface and the rubber of the tyre. Temperature and humidity or rain has a huge impact on the performance of the tyre. High ambient temperature does not affect the heat generated by the tyre but it does affect the heat dissipation, which causes the tyre to reach higher temperature levels, which could lead to greater tyre wear,[23].

Rainfall can actually reduce wear, because the water on the road acts as a lubricant between the road and the tyre. It also reduced the amount of tyre/road friction and increases the risk of the aquaplaning. This phenomenon occurs when the tyres loose contact with the road surface due to the development of a thin water layer on the whole contact area. This is usually the effect of high vehicle speeds, a thick water layer and insufficient tyre treading, [24].

2.4.7 Material composition and hardness

The material of both the road and the tyre play a large role in both wear and friction in the contact area. A soft tyre will wear faster but will have better traction than a harder tyre. Roads are often either concrete or asphalt. Concrete lasts longer, is more expensive and has lower friction coefficient than asphalt. Asphalt on the other hand is cheap and recyclable but does not last as long, [25].

2.5 Tyre and wear models

In this section a couple of tyre and wear models will be reviewed.

2.5.1 Tyre models

The purpose of the tyre model was to, with given input variables, determine the forces, moments and deformations acting on the tyre at any given time. There are several viable tyre models in existence with varying accuracy and complexity which can achieve this. The models can be separated into four different types which is displayed below in Figure 2.13.

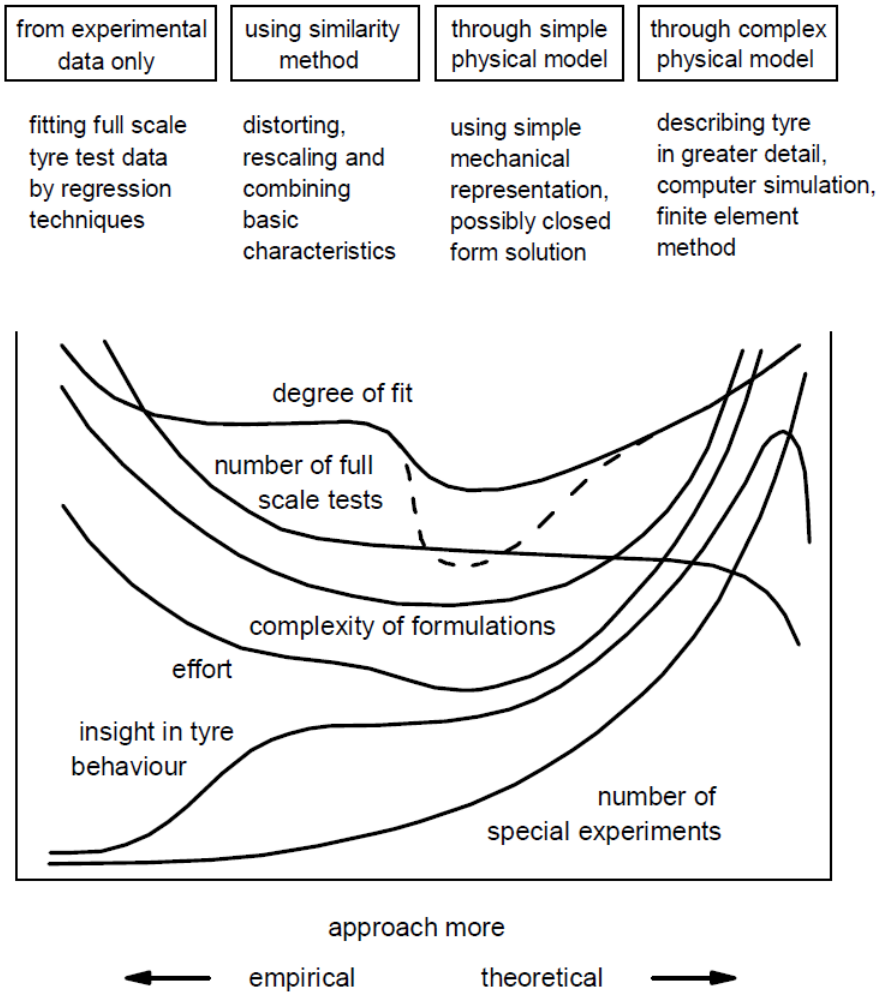

Figure 2.13: Four categories of possible tyre model approaches, [26].

The left-most category in Figure 2.13 represents the mathematical tyre models which describe measured tyre characteristics through tables or mathematical formulas. The formulas are derived by studying the data points and with the aid of regression procedures a best fit curve is created to fit the measured data. One of the more popular empirical models is the Magic Formula, [26].

The second category is referred to as using the similarity approach. This method utilizes measurements to obtain basic characteristics of the tyre. Through distortion, rescaling and multiplications, new relationships are obtained that can describe different conditions. This method is useful for application in vehicle simulation models that require rapid computations, [26].

The third category contains physical models, which through simple formulas provide a relatively accurate result. The models also have the added benefit of being easy to understand because of the physical assumptions made to create the necessary expressions. The most popular of the physical models is the brush model, which approximates the tyre with brushes stretching out from the carcass, [26].

The fourth category is focused on detailed on analysis of the tyre in both steady state and during transient behaviour, the finite element models belongs in this category. Assuming a rigid carcass significantly speeds up calculations and allows for a simpler mass spring model.

2.5.2 Wear models

The wear models investigated during the literature study are all related to adhesive wear, specifically abrasive wear. The motivation is that abrasive wear is the dominant component, compared to hysteresis wear, when studying short wear cycles. The models which have been reviewed are Archards wear law and a model based on Schallamach's theory.

Archards wear law

The wear law of Archard is a simple wear model. It expresses the general adhesive rubber wear as follows.

$$Q = K \cdot \frac{F_n \cdot s}{H} \tag{2.5}$$

where Q is the amount of wear expressed in m^3 and K is a dimensionless specific wear factor of adhesion and abrasion, F_n is the normal load in N, s the sliding distance in m and H is the hardness expressed in $\mathrm{N/m}^2$ of the material being worn away, [27]. The model provides a linear relation between the amount of wear and the sliding distance and normal load, [18].

Shallamach model

The model of Schallamach is similar to Archards wear law. The expression of Schallamach is focused on tyre wear and is defined as

$$A = \gamma \cdot s \cdot F_n \tag{2.6}$$

where A is the abrasive quantity, γ is the abrasion per unit energy dissipation, s is the sliding distance and F_n the normal force. The abrasive wear is then proportional to the sliding distance and normal force. For a more extensive review of the wear models refer to [18].

Chapter 3

Purpose of models and parameters of interest

Before choosing the appropriate models to study wear, it is convenient to first establish the area of application, requirements and limitations and also the accuracy and complexity required of the models. The merger of the suitable tyre model and wear model will yield a model which can predict accurate wear trends. This model will be referred to as the *Complete Model* or *CM*.

3.1 CM area of application

The area application of the CM is in simulations of new chassis concepts to reveal the best dynamic situation of the wheel-chassis unit to reduce the tyre wear and therefore increase the tyres life time.

3.2 CM requirements

The requirements where established to produce wear result which was as qualitatively correct as possible and with as little computational effort as possible. Furthermore, the models should be meant to increase the level of understanding, so models derived through physical expressions and relations where preferred over complex abstract models. No experimental setup was available, so no model using values or parameters that could only be obtained through experiments could be used. The CM should also be user friendly and easy to modify and improve.

3.3 CM limitations

The CM limitations would help determine which of the studied tyre, friction and wear models would be most suitable to use. As well as simplifying modelling, as some parameters have a small impact on wear yet large impact on complexity. In Table 3.1 the relevant limitations are listed in no particular order.

3.4 CM accuracy

The accuracy of the CM should be sufficient to see accurate trends in the behaviour of wear. The actual wear value is not likely to be accurate due to the simplifications and assumptions made.

Table 3.1: Delimitations of the CM

Nr	Limitation	Description
1	No temperature dependency	Both ambient and tyre temperature affect wear to large extents, as described in the literature study. The motivation for disregarding temperature dependency was to simplify the CM and reduce the computational effort.
2	Constant velocities	When using constant velocities some models will eventually reach a steady state condition. In this condition all forces and moments are constant which gives a more stable expression.
3	Infinitely stiff carcass	Assuming an infinitely stiff carcass leads to a simpler tyre model. It means that the tyre deformation only occurs in the tread of the tyre, which is convenient for calculation purposes. This is elaborated further in the derivation of expressions in the used tyre model.
4	Steady state conditions	Only evaluate wear in steady state conditions. Adding transient behaviour to the wear, although adding accuracy in predicting irregular tyre wear, is not required of the CM. It also adds computational effort.
5	Zero camber angle	The camber angle is kept at zero, although camber affects wear significantly the impact on computational effort and complexity of the CM is greatly increased, [9], which is why it is ignored.

3.5 CM complexity

The complexity should be kept at a level which the CM is understandable for a person with engineering background in vehicle mechanics.

3.6 Choice of tyre model

In the literature study four different categories of tyre models where presented, semi-empirical, similarity, physical and FE models. Two of these four categories where chosen for further investigation, these where the semi-empirical and the physical models. The motivation for this was that FE models where to complex and there was little literature referring to the similarity approach. The two remaining categories will be reviewed and then ranked.

Within the two model categories several different models exist. However, the general idea behind the models is the same. To determine which of the two categories best meet the requirements a ranking system was created. The category of model which reached the best agree-ability with the requirements stated above received the highest ranking. The two models categories are explained below.

3.6.1 Semi-empirical tyre models

Models in this category are generally based on empirical measurements and shape factors, peak values and other non dimensional coefficients, which determines the behaviour of the parameter. These parameters have no clear physical representation rather their purpose is to adapt a curve to the desired behaviour. An example of how an expression and figure containing these parameters is given below, [28].

The general form of the Magic Formula Tyre model for a given value of vertical load, F_z and camber angle,

γ, is given by

$$y = D \cdot \sin[C \cdot \arctan{(1 - E)Bx + E \cdot \arctan(Bx)}] \tag{3.1}$$

and

$$Y(X) = y(x) + S_V \tag{3.2}$$

$$x = X + S_H \tag{3.3}$$

where Y is the output and is defined as either the longitudinal force $F_x = y(\kappa)$ or the lateral force $F_y = y(\alpha)$. X is the input variable and κ and α are the longitudinal slip and side-slip angle respectively. The remaining variables are the various factors which scale, adapt and modifies the behaviour of the curve, which are explained below and displayed in Figure 3.1.

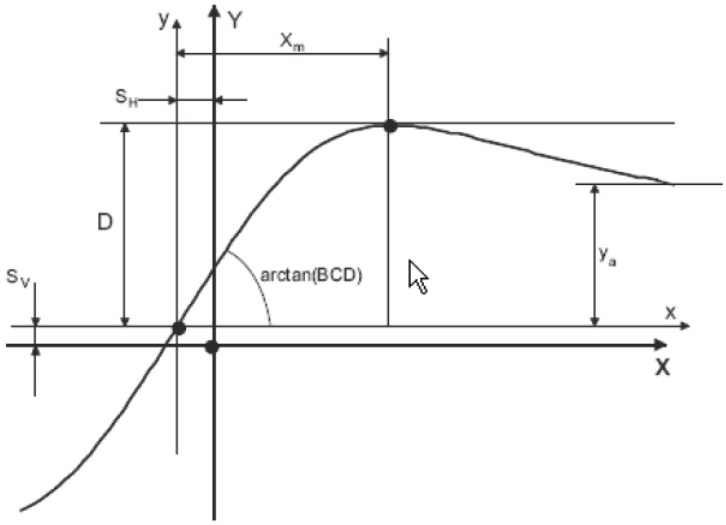

Figure 3.1: Magic Formula Tyre model parameters. B is the stiffness factor, C the shape factor, D the peak value, E the curvature factor, S_H the horizontal shift and S_V the vertical shift, [28].

The disadvantage of some empirical models are the empirical background which makes extending the models to include, temperature dependence, velocity related friction effect and tyre wear difficult. Doing so will most likely add to the already larger amount of input variables and shape factors, which will lead to increasing complexity and added computational effort. The empirical models are generally very accurate and the Magic Formula Tyre model is considered one of the most accurate tyre models. This is why it is so widely used in the automotive industry, [28]. Even though these models are generally quite accurate the computational effort required is rather low.

3.6.2 Physical tyre models

Models in this category tend to be more simple and have equations and expressions with a logical physical background. The brush tyre model is a common type of physical tyre model. It approximates the tyre as fitted on a rigid rim, with the tread modelled as springs, or bristles, which can deform in longitudinal, lateral and vertical direction. By following one bristle travelling through the contact area the forces and moments are calculated. Assuming a constant velocity the tyre will reach a steady state and so does the forces and moments. An illustration of how the tyre is modelled using the brush tyre model is displayed in Figure 3.2 and Figure 3.3 below.

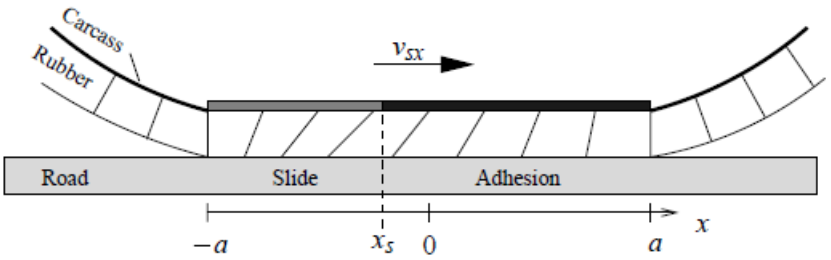

Figure 3.2: The deformation of the tread according to the brush model. The carcass has the velocity v_{sx} and the contact area with the vehicle velocity v_x.

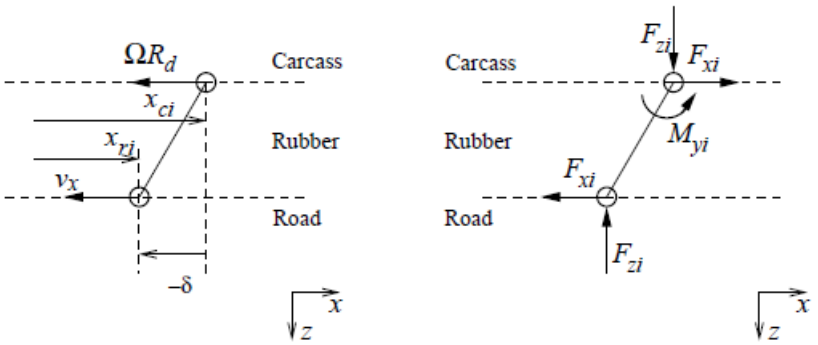

Figure 3.3: The relative velocity and upper and lower end of the bristle (left). Force equilibrium of the same bristle (right).

Physical tyre models have descent accuracy and doesn't require many input variables, as most equations and expressions are determined during the computational process. Most physical models are quite simple and thereby the computational effort required isn't large. The models are also adaptable to change and modifications to include effects and parameters not already present. Doing so will however add complexity and computational effort.

3.7 Tyre model ranking

In Table 3.2 the empirical and physical tyre models are ranked in order to determine which is the most suitable for the requirements stated earlier in Chapter 3, where 1 is a very poor fit and 5 is and excellent fit.

Table 3.2: Ranking of the tyre models

Statement	Physical model	Semi-empirical model	Motivation
Satisfying the area of application	4	4	There is no clear winner of this category since both of the models suit the area of application very well.
Meeting the requirements	4	3	The semi-empirical models are more quantitatively accurate than the physical model. It isn't valued as highly as the way the physical model explains and gives a deeper understanding of the tyre behaviour.
Limitations of the model	3	2	The physical model can be extended with less effort required than the semi-empirical models.
Accuracy of the model	2	4	The semi-empirical models are far more accurate than the physical models since the resulting curve is fitted to meet the requirements stated.
Simplicity of the model	3	2	The physical model is easier to comprehend given the physical background it stems from. This makes it more suitable for studying tyre behaviour compared to the semi-empirical models. Which generally are simple, but may be difficult to grasp since the scaling factors have no physical interpretation.
Summing	16	14	The semi-empirical models are generally more accurate but lack the ability to adequately physically represent the tyre, which is why the physical model is chosen.

The chosen tyre model category is the physical model. This model fits well with the requirements of the CM. In the physical model category one model type is particularly interesting, this is the brush tyre model. It fits the CM requirements very well, additionally an already working model of this model type was at the authors disposal, making it the obvious choice.

3.7.1 Choice of wear model

As stated in the literature study the wear model of Archard is more appealing to use given the requirements on the CM stated above. The Schallamach model does also possess accurate wear rates, but is a bit more complex and does include factors affecting wear which are not measured or taken into account in the thesis.

Chapter 4

Method

This chapter focuses on describing how the tyre and wear model are defined and implemented in MATLAB. Starting with deriving the brush equations and expressions for the tyre model followed by the wear model equations. The models are then combined and presented in the form of block diagrams.

4.1 Description and implementation of the CM

The purpose of the CM was to determine wear as a function of the forward velocity, side-slip angle, tyre inflation pressure, longitudinal slip and vertical load. These parameters are most significant at affecting wear, according to the literature study in Chapter 2.

4.1.1 Description of tyre model

The purpose of the tyre model was to, with given input variables, determine the forces, moments and deformations acting on the tyre at any given time as illustrated in Figure 4.1. To achieve this the tyre model would have to calculate the variables for specified in Figure 4.1 for each bristle element for every time step.

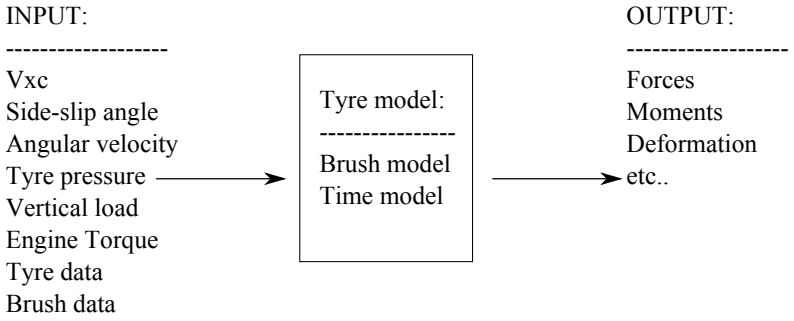

Figure 4.1: Desired input and output for the tyre model.

Initial conditions and tyre kinematics

The *brush tyre model* or *BM*, is a part of the CM and it calculates the deformations and forces exerted on each bristle in the tyre. Before this could be achieved the tyre data, the initial conditions of the car and the velocities needed to be defined. The tyre data consists of the parameters specified in Table 4.1.

Table 4.1: Tyre parameters for the brush tyre model.

f_{z0}	Nominal tyre load
n	Number of bristles
sa	Segment angle
d_{px}	Longitudinal bristle damping per unit length
d_{py}	Lateral bristle damping per unit length
d_{pz}	Vertical bristle damping per unit length
c_{px}	Longitudinal bristle stiffness per unit length
c_{py}	Lateral bristle stiffness per unit length
c_{pz}	Vertical bristle stiffness per unit length
R_w	Unloaded tyre radius
p_t	Normalized tyre inflation pressure

The segment angle is only used to define the angle in where the bristles are travelling, illustrated in Figure 4.3. The segment angle is divided into n equally spaced segment, one for each bristle element. Naturally, increasing the segment angle while keeping the number of bristles constant will reduce the number of bristles in contact with the road since it increase the space between the bristles. This gives a less accurate result than having a narrower sa. The minimum segment angle should be defined so that the contact angle created by the tyre deformation never exceeds the segment angle.

The tyre inflation pressure in the thesis is normalized, meaning it is the ratio between the current tyre pressure and the ideal tyre pressure. The motivation behind this is that it allows for a linear relation between the normalized tyre inflation pressure p_t and the vertical bristle stiffness $c_{pz,d}$ as described in Equation 4.1 and 4.2. This approximation is based on the assumption that small variations of the tyre inflation pressure do not alter the tyre–road contact geometry, other than the length of the contact area. It is therefore assumed that the tyre inflation pressure is only valid ± 20 % from the ideal tyre pressure. The new vertical bristle stiffness is defined as

$$c_{pz} = c_{pz,d} \cdot \frac{p_{t,current}}{p_{t,ideal}} \tag{4.1}$$

and

$$0.8 \cdot c_{pz,d} \leq c_{pz} \leq 1.2 \cdot c_{pz,d} \tag{4.2}$$

where c_{pzd} is the default bristle stiffness, $p_{t,current}$ is the current tyre inflation pressure and $p_{t,ideal}$ is the ideal tyre inflation pressure. Increasing the bristle stiffness simulates an increase in tyre inflation pressure and decreasing the bristle stiffness simulates a decrease in tyre inflation pressure.

The initial conditions of the car were required to determine how the mass-spring system, between the road, tyre and the strut system of the car, behaved over time. The mass-spring system is modelled as a quarter car system, illustrated in Figure 4.2, below.

Each bristle is represented by a spring and damper. The notations in Figure 4.2 are defined as specified in Table 4.2. The velocities of the wheel center where chosen to start at $v_x = 5$ m/s and $v_y = 0$ m/s. The motivation for this was to create a reference wear case using these settings.

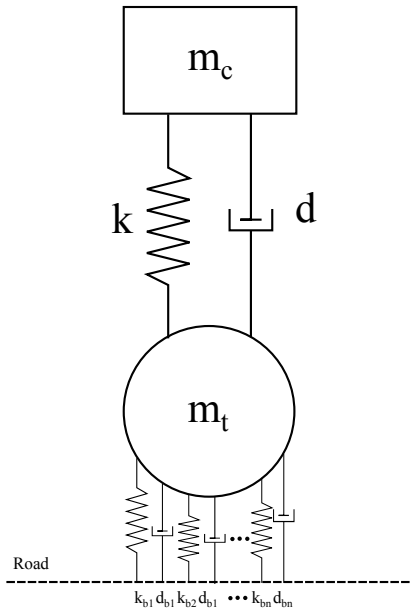

Figure 4.2: Model of the road-vehicle interaction

Table 4.2: Explanation of notations in Figure 4.2

m_c	Quarter car mass (sprung mass)
m_t	Tyre mass (unsprung mass)
k	Strut spring stiffness coefficient
d	Strut damping coefficient
k_{bn}	Spring stiffness coefficient of the $n:th$ bristle element
d_{bn}	Damping coefficient of the $n:th$ bristle element.

Bristle deformation

The deformation of the tyre is the sum of all individual bristle deformations in each direction. The following equations determine the deformations and forces arising in the $i:th$ bristle. In Figure 4.3 the geometry and the derivation of the bristle deformation in the vertical direction is explained.

Using Figure 4.3 the deformation in the vertical direction for the $i:th$ bristle could be defined as

$$\delta_z(i) = z_t - \cos(\phi(i)) \cdot R_w \tag{4.3}$$

where z_t indicates the loaded tyre radius, ϕ_i is the angle from the center line to the $i:th$ bristle and R_w is the unloaded wheel radius. The i indicates which bristle is currently being calculated, up to n, the total number of bristles. The same geometric principle as above is applied to the $i:th$ longitudinal and lateral bristle yielding the deformations

$$\delta_x(i) = \Omega \cdot \Delta t \cdot R_w \cos(\phi(i)) - v_x \cdot \Delta t \tag{4.4}$$

$$\delta_y(i) = -v_y \cdot \Delta t - R_w \sin(\phi(i))\dot{\alpha} \cdot \Delta t. \tag{4.5}$$

These deformations where then used to calculate the forces acting on each bristle using the stiffnesses from the tyre data:

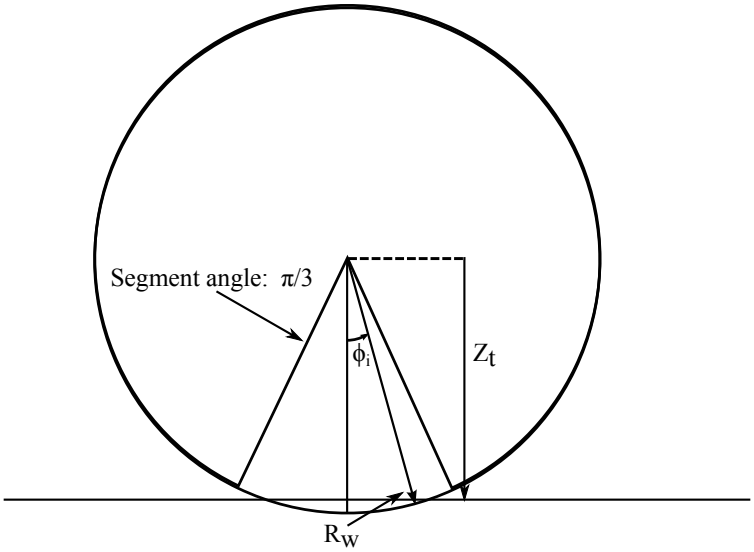

Figure 4.3: Geometric relation for deriving the vertical bristle deformation, including segment angle.

$$f_x(i) = \delta_x(i) \cdot c_{px} \tag{4.6}$$

$$f_y(i) = \delta_y(i) \cdot c_{py} \tag{4.7}$$

The resultant force vector could then be derived using Equations 4.6 and 4.7

$$\bar{f}(i) = \sqrt{(f_x(i))^2 + (f_y(i))^2} \tag{4.8}$$

The bristle force vector is limited to the friction limit of the tyre/ground contact according to

$$\bar{f}(i) \leq \mu \cdot f_z(i) \tag{4.9}$$

where μ is the friction coefficient and $f_z(i)$ is the vertical force on the $i : th$ bristle which is determined by the initial conditions. If the friction limit in equation 4.8 is exceeded the bristle is sliding. The new force component in x – and y – direction is then

$$f'_x(i) = \frac{f_x(i) \cdot \mu f_z(i)}{\bar{f(i)}} \tag{4.10}$$

and

$$f'_y(i) = \frac{f_y(i) \cdot \mu f_z(i)}{\bar{f(i)}}. \tag{4.11}$$

Equations 4.10 and 4.11 represents the new force component in x– and y–direction limited to the friction limit. The sliding work can be calculated using

$$w_x(i) = |f'_x(i) \cdot (\delta_x - \frac{f'_x(i)}{c_{px}})| \tag{4.12}$$

$$w_y(i) = |f'_y(i) \cdot (\delta_y - \frac{f'_y(i)}{c_{py}})| \tag{4.13}$$

Equations 4.4 to 4.13 are then used to calculate the sum of forces, moments and work for all bristles up to the $n:th$ bristle. This results in the following forces

$$F_x = \sum_{i=1}^{n} f_x(i) \tag{4.14}$$

$$F_y = \sum_{i=1}^{n} f_y(i) \tag{4.15}$$

$$F_z = \sum_{i=1}^{n} f_z(i) \tag{4.16}$$

moment

$$M_z = \sum_{i=1}^{n} f_y(i) \cdot R_w \sin\phi(i) \tag{4.17}$$

and work

$$W_x = \sum_{i=1}^{n} w_x(i) \tag{4.18}$$

$$W_y = \sum_{i=1}^{n} w_y(i). \tag{4.19}$$

Time stepping

The forces, moments and work calculated in the BM are stored in the *TM, Time Model*. Using the data from the BM, the TM calculates the vertical behaviour of the car and tyre, the contact length, effective rolling radius and the pressure distribution. It then adds an increment of time Δt for the BM to calculate the new forces and moments. The iteration is repeated until the TM has reached the end time t_{stop}. The TM can be described as a link between the behaviour of the tyre and the car. The simulation time is always 2 seconds, but the evaluation starts after 1 second. The motivation behind this is that it allows for the model to reach a steady state, which is crucial. The wear model would otherwise possibly display strange oscillations or other faulty results. The steady state was confirmed by verifying that the wheel speed, $\dot{\theta}$, the vertical position of the tyre, z_t and the longitudinal force F_x had reached a steady state. For the longitudinal force a steady state would mean a linearly increasing curve while the wheel speed and vertical position of the tyre would yield a curve which time derivative is zero.

Before calculating the vertical behaviour of the car and tyre the suspension forces are needed to be calculated.

$$F_s(j+1) = k(z_t(j) - z_c(j)) + d(\dot{z_t}(j) - \dot{z_c}(j)) \tag{4.20}$$

where z_t and $\dot{z_t}$ is the loaded tyre radius and vertical velocity of the tyre, z_c and $\dot{z_c}$ is the vertical displacement and velocity of the car and k and d are the spring stiffness and damping of the suspension of the car. The index j represents the $j:th$ time step and the index $j+1$ is $j:th$ time step plus one. The behaviour of the car is then calculated as follows

$$\ddot{z_c}(j+1) = \frac{F_s(j+1)}{m_c} - g \tag{4.21}$$

$$\dot{z_c}(j+1) = \dot{z_c}(j) + \ddot{z_c}(j+1) \cdot \Delta t \tag{4.22}$$

$$z_c(j+1) = z_c(j) + \dot{z_c}(j+1) \cdot \Delta t \tag{4.23}$$

and the behaviour of the tyre is calculated in the same fashion

$$\ddot{z_t}(j+1) = \frac{F_z(j+1) - F_s(j+1)}{m_t} - g \tag{4.24}$$

$$\dot{z_t}(j+1) = \dot{z_t}(j) + \ddot{z_t}(j+1) \cdot \Delta t \tag{4.25}$$

$$z_t(j+1) = z_t(j) + \dot{z_t}(j+1) \cdot \Delta t. \tag{4.26}$$

where $\ddot{z_c}$ and $\ddot{z_t}$ are the vertical accelerations of the car and tyre. An additional set of equations is designed to deal with what is called wheel dynamics. The purpose of these equations is to adjust the wheel speed of the tyre to match the desired velocity.

$$\ddot{\theta}(j+1) = \frac{M_e - z(j) \cdot F_x(j+1) + M_y(j+1)}{J} \tag{4.27}$$

$$\dot{\theta}(j+1) = \dot{\theta}(j) + \ddot{\theta}(j+1) \cdot \Delta t \tag{4.28}$$

$$\theta(j+1) = \theta(j) + \dot{\theta}(j+1) \cdot \Delta t \tag{4.29}$$

where $\ddot{\theta}$, $\dot{\theta}$ and θ are the wheel acceleration, wheel speed and wheel rotational angle respectively. The M_e is the engine torque, the $z(j) \cdot F_x(j+1)$ is the torque derived from the bristles, M_y is the wheel torque and J is the inertia of the tyre. The engine torque is essential when determining longitudinal slip, by adjusting the engine torque in Equation 4.27 different levels of longitudinal slips can be simulated. This is achieved at constant velocity.

The contact length of the tyre/ground is $2a$. This can be realized by assigning the angle Γ as the angle between the loaded tyre radius z_{te} extended vertically from the center of the tyre to the road and the unloaded tyre radius at the edge of the contact area R_w. The angle was used to calculate the length a by using the previous statements as follows

$$\Gamma = \arccos\left(\frac{z_{te}}{R_w}\right) \tag{4.30}$$

and

$$a = z_t \cdot \tan\Gamma \tag{4.31}$$

where a represents half the contact area, so the full contact area is $2a$. The wheel torque M_y can be calculated using the product of the loaded tyre radius and the longitudinal forces

$$M_y = F_x \cdot z_t \tag{4.32}$$

The pressure distribution in the contact patch is commonly described by a parabolic function, in this case determined using the non zero values of Equation 4.3, combined with Equation 4.31 and the steady state value of the vertical forces, F_{ze}.

$$q_{zx} = \frac{3F_{ze}}{4a}\left(1 - \left(\frac{x}{a}\right)^2\right) \tag{4.33}$$

The Equations 4.20 to 4.33 are stored for every time increment Δt and then evaluated for the desired input parameters in the *Parameter model, PM*.

Parameter model

In this model the calculations performed in the BM and TM are evaluated for the input parameters specified in Table 4.3.

Table 4.3: Evaluated input parameters.

v_x	Forward velocity of the wheel center
α	Side-slip angle
Ω	Angular velocity of the tyre
$mass$	Mass of the quarter car and tyre
p_t	Tyre inflation pressure
M_e	Engine torque

The parameters are evaluated separately and in pairs, in order to simulate various driving conditions. The results from the BM and TM are stored in this model. This is where the wear equation is introduced.

4.1.2 Description of wear model

The Archard wear model is rather simple, but has proven to describe wear reasonably well. The wear law is described as follows

$$Q = K\frac{F_n \cdot s}{H} \tag{4.34}$$

where F_n is the normal force acting on the contact area, s is the sliding distance, K is a dimensionless wear constant and H is a constant representing the hardness of the material being worn. Based upon Reye's hypothesis the product $F_n \cdot s$ could be approximated as the friction work done in longitudinal and lateral direction. The hypothesis states that the volume of material lost due to adhesive wear effects is proportional to the work performed by the friction forces,[29]. Since K and H are constants this hypothesis holds for Equation 4.34 resulting in $F_n \cdot s \approx W_x + W_y$, where W_x and W_y is the friction work done in longitudinal and lateral direction. Using the new relation of friction work and rewriting 4.34 expressed in mm^3 leads to the expression.

$$Q = 10^9 \cdot K\frac{W_x + W_y}{H} \tag{4.35}$$

where Q is the wear in volume loss, now in mm^3, K is a dimensionless wear constant, W_x and W_y is the sum of friction work done in longitudinal and lateral direction and H is the hardness of the softest material of the road and rubber tyre. The parameter K represents the fraction of actual contact surface which is removed by the wear process and its value is between 10^{-3} to 10^{-9}, the higher the value the higher the friction, [30]. For this thesis the values of the dimensionless wear constant and hardness are chosen as $K = 10^{-9}$ and $H = 70$ N/m^2. The motivation for choosing the hardness is based upon [31], where the hardness is stated to be roughly 60 N/m^2. The value of K was chosen because it is the value which yields the lowest amount of wear while still being a valid.

Before the wear is calculated for the desired input parameters a reference wear case is chosen, which is needed to normalize the wear, using the input parameters in Table 4.4. The reference wear case is chosen arbitrarily as a general driving state. Using the engine torque of $M_e = 0$ Nm is equivalent to having zero longitudinal slip or $\lambda = 0$.

Table 4.4: Input parameters for the reference wear case

Parameter	Value	Unit
v_x	5	m/s
α	0	rad
f_{z0}	$9.82 \cdot 350$	N
p_t	1	–
M_e	0	Nm

The motivation for normalizing the wear is because the aim is to analyse the trend of the wear, not the actual value. The reference case is here after refereed to as Q_0, which is defined in Equation 4.36. The wear value stated in 4.36 is then used to normalize the other calculated values of wear, leading to a normalized dimensionless wear quantity, stated in Equation 4.37.

$$Q_0 = 10^9 \cdot 10^{-9} \frac{W_x + W_y}{70} = 4.63 \cdot 10^{-6} \text{ mm}^3/\text{m} \tag{4.36}$$

$$Q_n = \frac{Q_c}{Q_0} \tag{4.37}$$

where Q_n is the normalized wear, Q_c is the current wear and Q_0 is the reference wear. Determining the wear for the desired wear cases was an iterative procedure, where one set of input parameters where calculated, with an incremental increase at every iteration. The only parameter calculated in the wear model, before the wear calculations where performed, was the longitudinal slip, which is defined

$$\lambda = \frac{R_w\Omega - v_x}{\max(v_x, R_w\Omega)} \tag{4.38}$$

where the maximum of v_x and $R_w\Omega$ indicates if the tyre is braking or accelerating. If $R_w\Omega$ is larger then the tyre is accelerating, the most extreme case yields $\lambda = 1$, corresponding to 100% slippage. If v_x is larger then the tyre braking, the most extreme case yields $\lambda = -1$, the wheel is locked and there is 100% slippage.

The relevant equations for determining wear are now defined. With the models completed it is appropriate to illustrate the interaction of them in MATLAB, this is displayed in the next section.

4.2 The complete model in MATLAB

The interaction between the brush tyre model, time model, parameter model and the wear model in MATLAB are displayed in Figure 4.4.

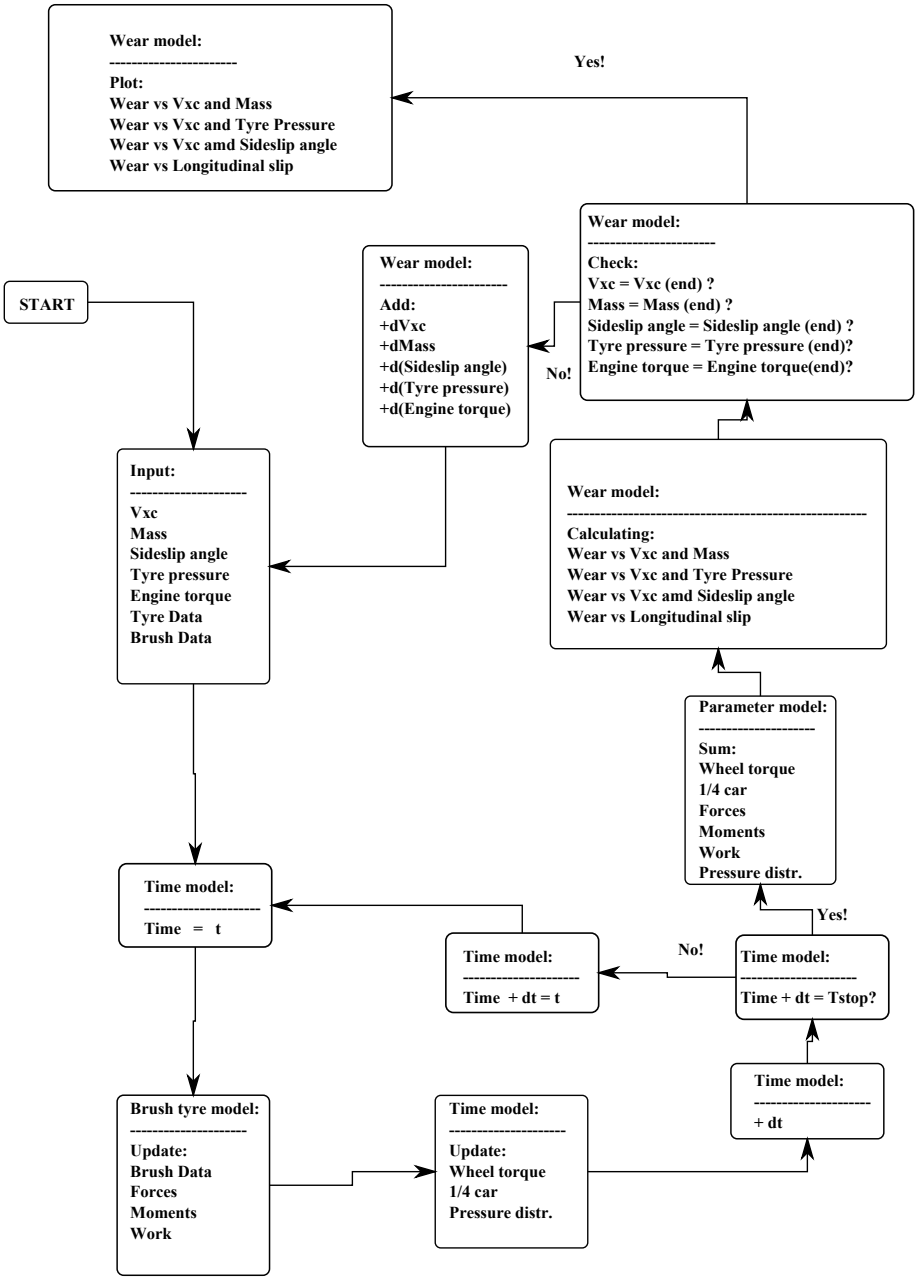

Figure 4.4: Flowchart of the CM in MATLAB.

The model starts at *start* with the predetermined inputs for the BM at time t. The BM calculates the bristle deflections, forces, moments and work, for all bristles, which is then stored for the time model. The TM updates the wheel torque, quarter car conditions and then adds a time increment, storing the previous conditions as input conditions for the next iteration of the BM. It then checks if has reached the end time t_{stop}, if not then it continues to iterate the BM and TM data until it has. If it has, the data from the BM and TM are summed and stored to the PM. The wear model uses the stored summed data from the PM for the current input data. It then checks if swept input parameters have reached there final value. If not, the swept parameters gains an incremental increase which is stored as the new input for the BM and TM. If yes, the wear model plots the wear as a function of the swept parameters.

Chapter 5

Results and discussion

The results of the CM are illustrated for wear as a function of both one and two swept input parameter. In the first section the wear is plotted as a function of one input parameter, followed by a validation and discussion for each parameter. The second section contains the wear plots as a function of two input parameters, which are then discussed and verified.

The wear derived in this thesis is compared to validation figures, which are results gathered from references,[32] and [33]. The results from these sources are not measurement data, so their accuracy might not be sufficient for determining the exact error or fit. However, the purpose is to determine whether or not the trend matches with these validation results. Measurement data would have to be obtained by conducting own experiments or tests which were not available at the time of the thesis.

The wear results produced by the CM are dimensionless, but the unit of the reference wear and current wear are measured in mm^3/m or volume wear loss due to sliding per unit length that the wheel travels.

5.1 Wear as a function of forward velocity

The wear as function of the forward velocity is illustrated in Figure 5.1. The results in Figure 5.1 show that the wear increases exponentially as the velocity increases. In addition to this an oscillating behaviour with increasing amplitude as the velocity increases is also noticeable. The blue curve illustrates the curve fitting of the wear results, or the trend of the red curve. The reason for the oscillations is most likely due to numerical errors. Both the calculated curve and the curve fitting of the calculated curve is illustrated in Figure 5.1, but subsequent figures only contain the curve fitted plots, unless the calculated results do no contain any oscillations. The motivation behind this is that, if oscillations are present, the curve fitting more clearly illustrates the wear trend.

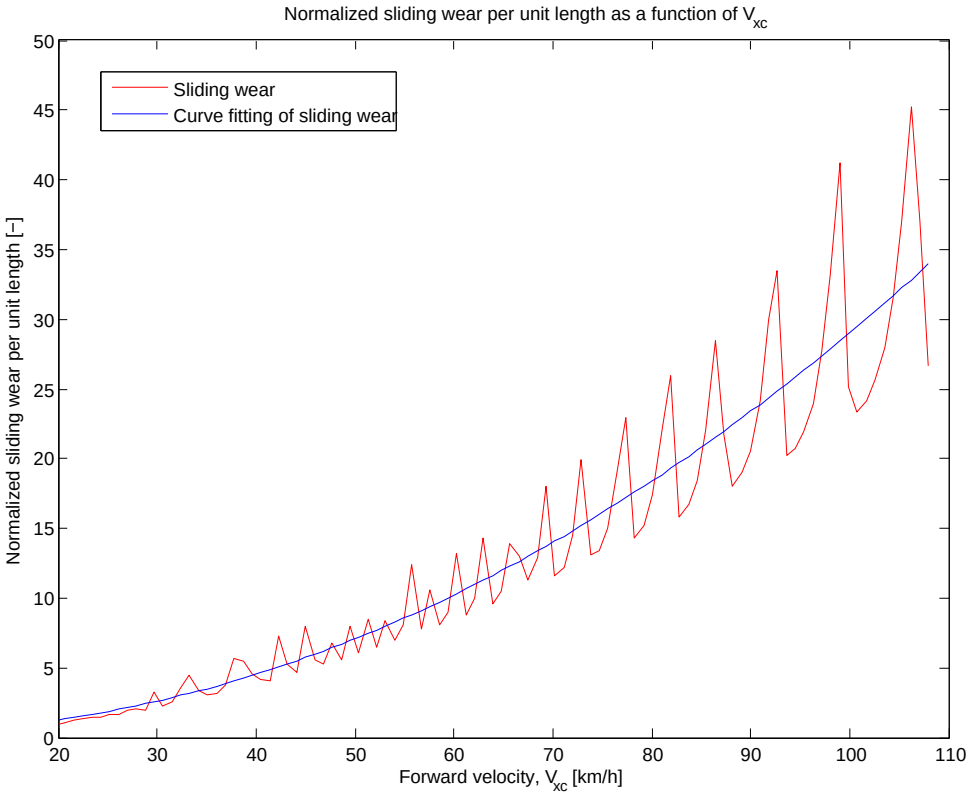

Figure 5.1: Normalized wear as a function of the forward velocity. The blue curve represents the sliding wear calculated with the model and the red curve represents an approximation of the blue curve using a least squares method of fitting. For this wear case the input parameters are fixed at the Q_0 values, meaning $p_t = 1$, $\alpha = 0°$, $M_e = 0$ Nm and $f_{z0} = 350 \cdot 9.82$ N.

The actual wear in Figure 5.1 increases exponentially with increasing velocity and at the same time oscillating with increasing amplitude as the velocity increases. The reason for this behaviour was first thought to be the cause of low damping, which would yield this type of behaviour. Tests where run but disproved this theory. Other possible theories was to either decrease the time steps, yielding a more detailed plot, or delay the evaluation time, perhaps giving the model enough time to reach steady state before starting the measurement. Decreasing the time step increases the computational effort required to the point at which the model could not be run, which lead to this theory being abandoned. Delaying the evaluation time yielded no change in the results since the model had already reached a steady state condition. Perhaps the most reasonable explanation would be an erroneous numerical approximation in the model.

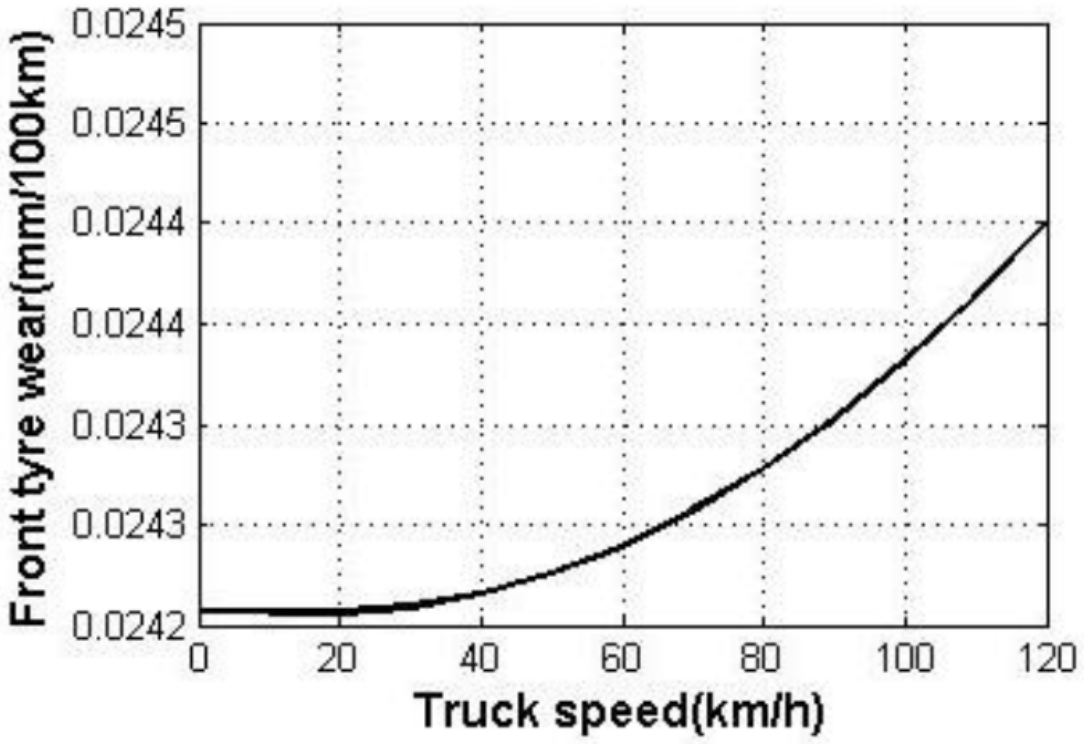

Figure 5.2: Wear as a function of the forward velocity, used for validation, [32].

The results illustrated in Figure 5.2 are the validation results, which where obtained by simulation not measurements. Comparing the validation results in Figure 5.2 with the results in Figure 5.1 it can be seen that the trends match reasonably well. The trend of the results in Figure 5.1 is illustrated by the red curve, which is of exponentially increasing behaviour as the the forward velocity increases. Assuming that the red curve in Figure 5.1 is a good approximation of the trend of the wear a comparison can be made with the validation results in Figure 5.2. The validation results and the CM results are illustrated in mm/100km and - respectively. In order to compare the two results a reference wear case for the validation results was created at 5 m/s, corresponding to 18 km. At this velocity in Figure 5.2 the wear is 0.0242 mm/100km meaning this would indicate the reference wear, using the same principal as in the thesis. At 110 km/h the normalized wear in validation figure would then be $0.02445/0.0242 = 1.0103$, compared to the CM results of $35/1 = 35$. The value difference could possibly be minimized by iterating a new value of the Archard's law parameter K which fits the validation figure better. It should also be emphasized that the validation results are not measurement results, but rather the result of a simulation. It is therefore difficult to determine the correctness of the values in the validation. However, it is plausible that the trend of both the validation results and the results illustrated in Figure 5.1 is correct, since the trend of the wear in both cases is exponentially increasing as the velocity increases.

5.2 Wear as a function of side-slip angle

The side-slip angle is defined as the angle between the longitudinal and lateral velocity component. The wear as a function of the side-slip angle is illustrated in Figure 5.3.

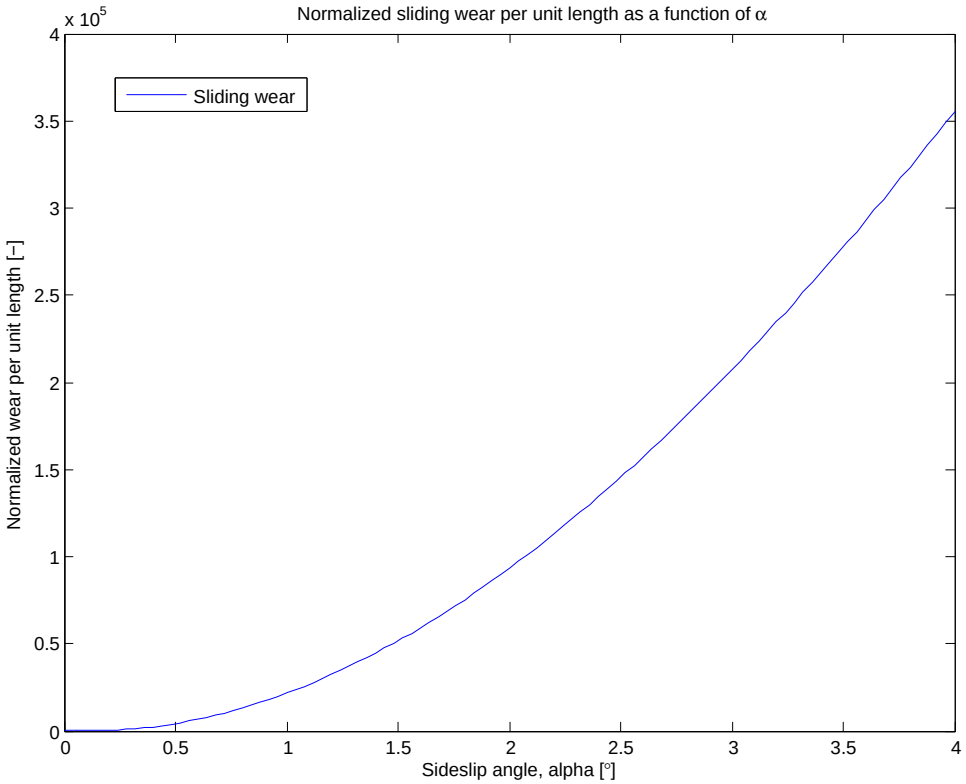

Figure 5.3: Normalized wear as a function of the side-slip angle. For this wear case, the input parameters are fixed at the Q_0 values, meaning $p_t = 1$, $v_x = 5$ m/s, $M_e = 0$ Nm and $f_{z0} = 350 \cdot 9.82$ N.

The results in Figure 5.3 show that wear is greatly affected by the side-slip angle. This is natural of course and compared to the most severe wear cases in Figure 5.4 its larger. This can be concluded by studying the validation figure and identifying, for example, the most severe wear case, which seems to be the D tyre. In the Figures 5.4 it is difficult to determine the wear at 0° side-slip angle, the reference wear is therefore measured at 1°, where it's estimated, using a ruler, to be 1 mm/1000km. This wear value is used as a reference case to determine the normalized wear for 2°, 3° and 4°. The wear, for the respective angles is approximated to $W_{n,2^\circ} = 7$, $W_{n,3^\circ} = 17$ and $W_{n,4^\circ} = 36$. Comparing these normalized wear value with the ones in Figure 5.3, using the wear value at 1° to normalize, it can be determined that the slope of the curve in validation figure is not as steep as in the result in the thesis. However, the most important characteristic of the curve in Figure 5.3 is the trend, which is similar to many of the curves in Figure 5.4, indicating a realistic trend.

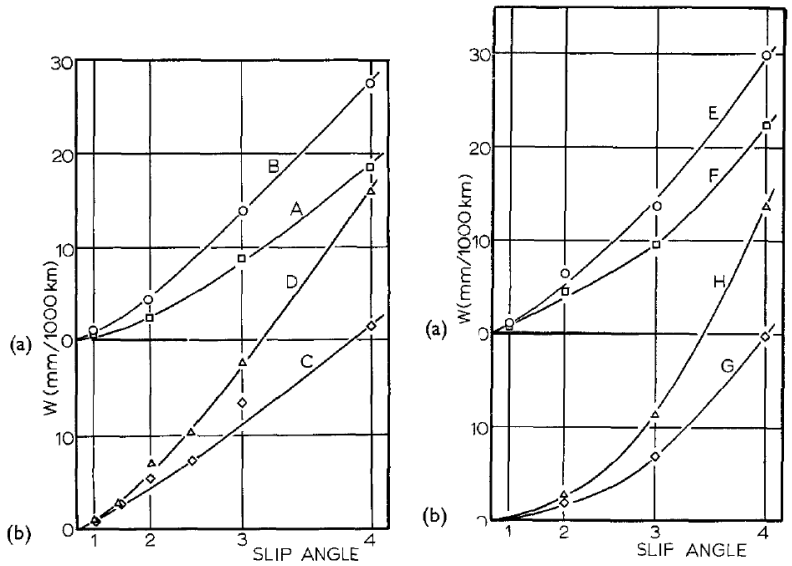

Figure 5.4: Wear as a function of side-slip angle for various tyre brands, with $f_{z0} = 4583$N and $v_x = 13.41$m/s, [33].

5.3 Wear as a function of vertical bristle stiffness

The tyre inflation pressure is simulated by the vertical bristle stiffness, as mention in Chapter 4 Description of tyre model. The tyre inflation pressure is measured in a normalized scale and is assumed to only be valid for $\pm 20\%$ from the ideal tyre pressure $p_t = 1$. Beyond these values the increased/reduced stiffness is assumed to alter the contact geometry non-linearly. The wear as a function of the tyre inflation pressure is illustrated in Figure 5.5.

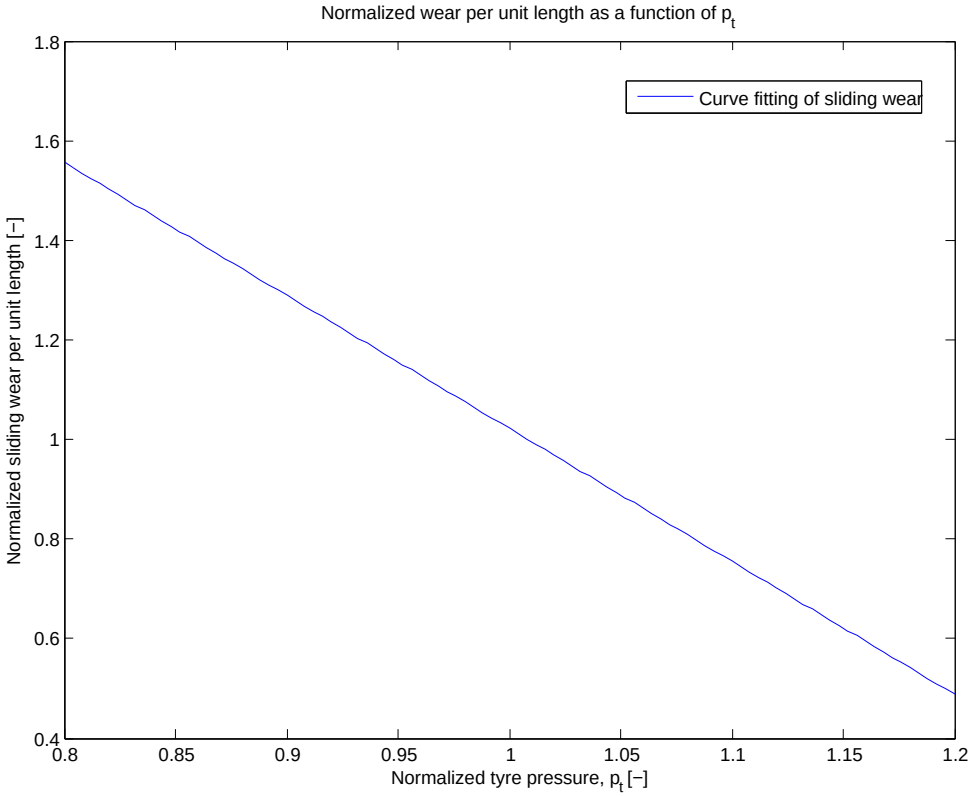

Figure 5.5: Normalized wear as a function of the tyre inflation pressure. The curve illustrates a linear approximation of the results. For this wear case the input parameters are fixed at the Q_0 values, meaning $\alpha = 0°$, $v_x = 5$ m/s, $M_e = 0$ Nm and $f_{z0} = 350 \cdot 9.82$ N.

The trend of the wear curve in Figure 5.5 and Figure 5.6 are the same, reduced wear for higher tyre inflation pressure. However, the results showed a oscillating behaviour, so a linear approximation was used instead, illustrated in Figure 5.5. The reason for this behaviour is thought to be the same as the reason behind the oscillations in Figure 5.1, wear as a function of the forward velocity. Meaning it is likely due to numerical errors caused while iterating.

The curve in Figure 5.5 is assumed to be valid for $\pm 20\%$ from the reference value of $p_t = 1$, the results in Figure 5.6 need to be subject to the same restrictions. The motivation behind this is that altering the stiffness or tyre inflation pressure further would alter the contact geometry. Figures 5.5 and 5.6 where compared by

firstly determining the optimal or reference tyre pressure for the validation figure, then the range of ±20% from that reference value. In Figure 5.6 the reference inflation pressure is indicated by the asterisk, circle and diamond, corresponding to roughly 125 psi. Which yields the minimum and maximum tyre inflation pressure 100 psi and 150 psi, respectively. Approximating the validation curve, in this region, and the thesis curve as straight lines allows for a comparison to be made between the start and end values of both curves. The difference of the curve in Figure 5.5 is $p_{t,0.8}/p_{t,1.2} = 3$ and for the validation curve in Figure 5.6 $p_{t,100}/p_{t,150} = 1.0333$. The difference between the curves in Figures 5.5 and 5.6 is then $3/1.0326 \approx 3$. Showing that approximating the tyre inflation pressure linearly with the bristle stiffness yields a sufficiently accurate wear trend.

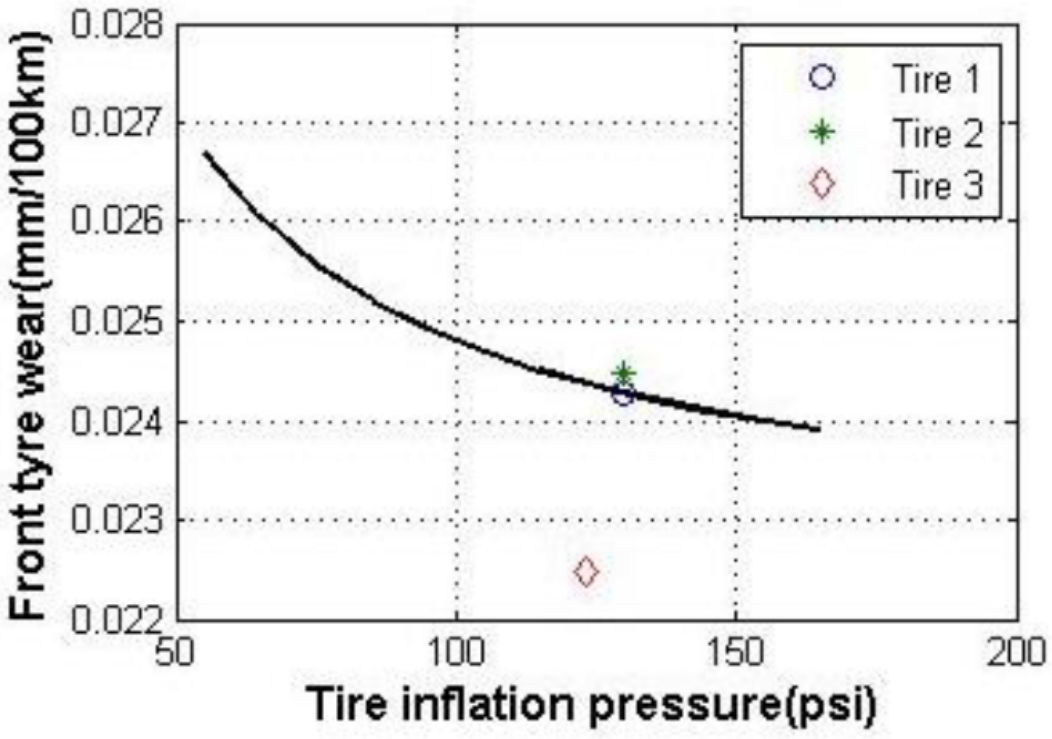

Figure 5.6: Wear as a function of the tyre inflation pressure, used for validation,[32].

5.4 Wear as a function of longitudinal slip

Longitudinal slip occurs when the forward velocity of the vehicle and the product of the tyre velocity the tyre radius don't match. Slip condition occur either when braking or accelerating. In the extreme braking condition, locked wheels yet still moving forward, the value of the longitudinal slip reaches $\lambda = -1$. For the extreme acceleration condition, standing still while the tyre is spinning, the value of the longitudinal slip reaches $\lambda = 1$. However in Figure 5.7 the segment $-0.3 \leq \lambda \leq 0.3$ is illustrated. This is meant to represent common occurrences of longitudinal slip while driving.

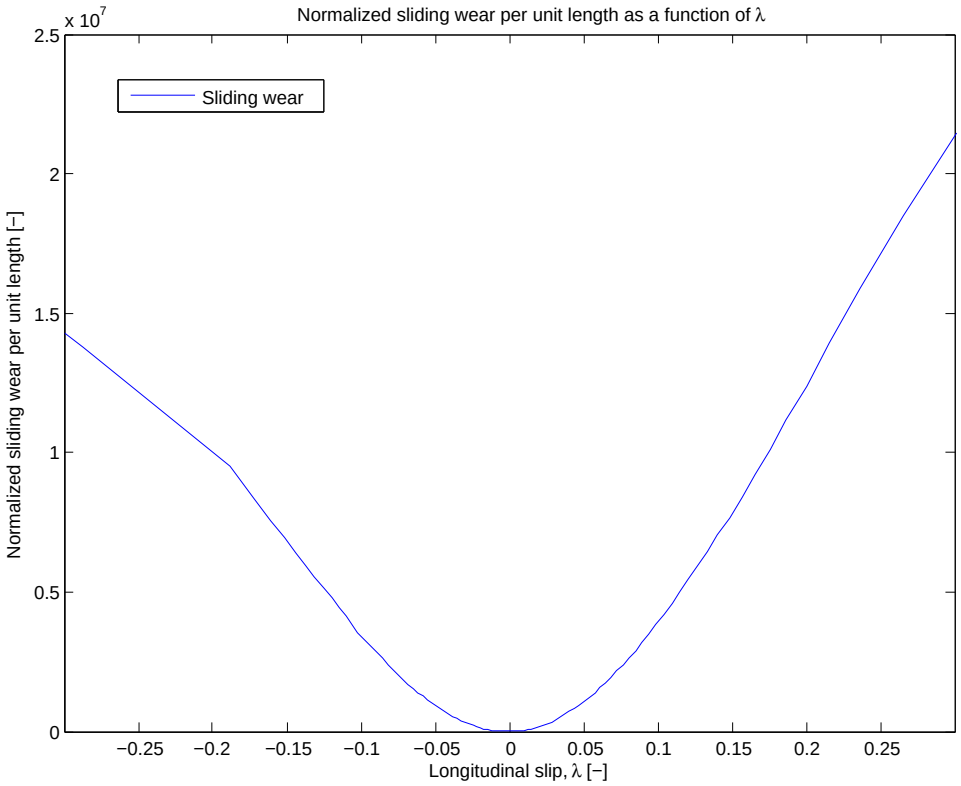

Figure 5.7: Normalized sliding wear as a function of longitudinal slip. For this wear case the input parameters are fixed at the Q_0 values, meaning $v_x = 5\text{m/s}$, $\alpha = 0\,^\circ$, $p_t = 1$ and $f_{z0} = 350 \cdot 9.82$ N.

Comparing the curve trend to the left and right of the origin in Figure 5.7 it can be seen that the behaviour of the wear are roughly the same for acceleration and braking. The reason for the slight difference is; the braking case is helped by the friction moment of the road to eventually stop the vehicle. Unfortunately finding validation plots of wear results as a function of the longitudinal slip is difficult. However referring to [26] and [9] the trend of wear as a function of longitudinal slip seems to be accurate. Meaning that wear increases as the longitudinal slip increases. If future measurement results show that the wear rate is far to high/low, the results could be fitted to the desired values by optimizing the wear parameter K. Increasing K would increase the wear while decreasing it would lower the wear.

5.5 Wear as a function of vertical load

The vertical load on the tyre contact area is always present, since the tyre it self has a mass. The load on the tyre in this thesis is a quarter of the cars total mass. The wear as a function of the vertical load is illustrated in Figure 5.8.

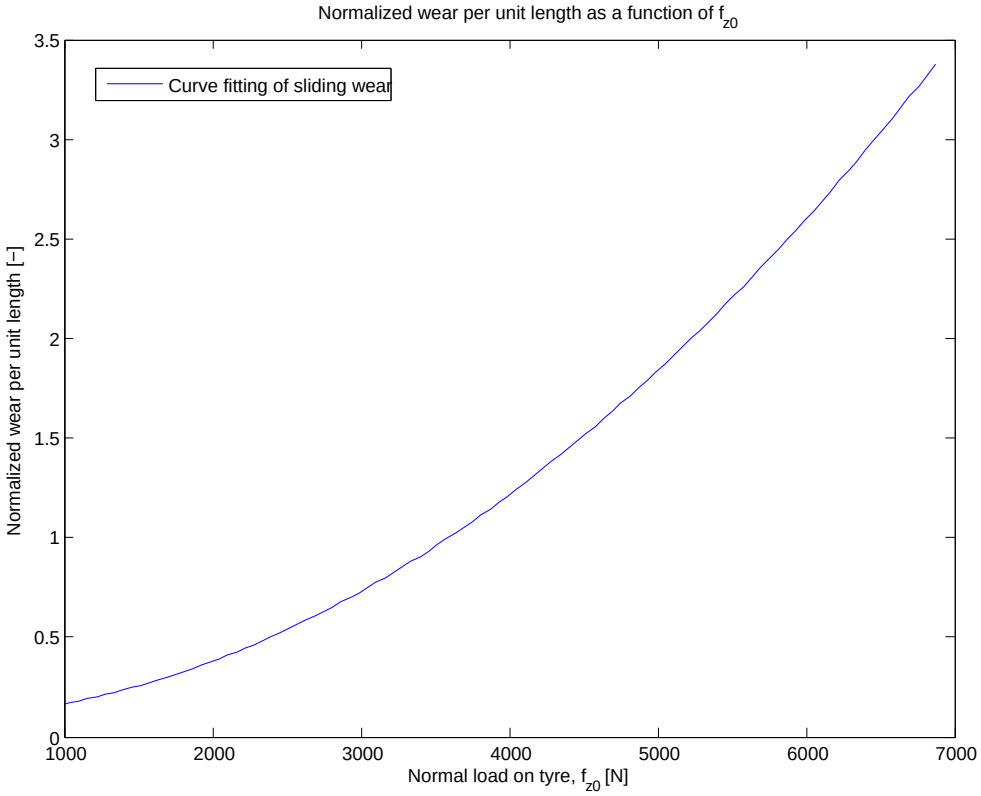

Figure 5.8: Normalized wear as a function of vertical load. The curve illustrates a curve fitting of the results. For this wear case the input parameters are fixed at the Q_0 values, meaning $\alpha = 0°$, $M_e = 0$ Nm and $v_x = 5$ m/s

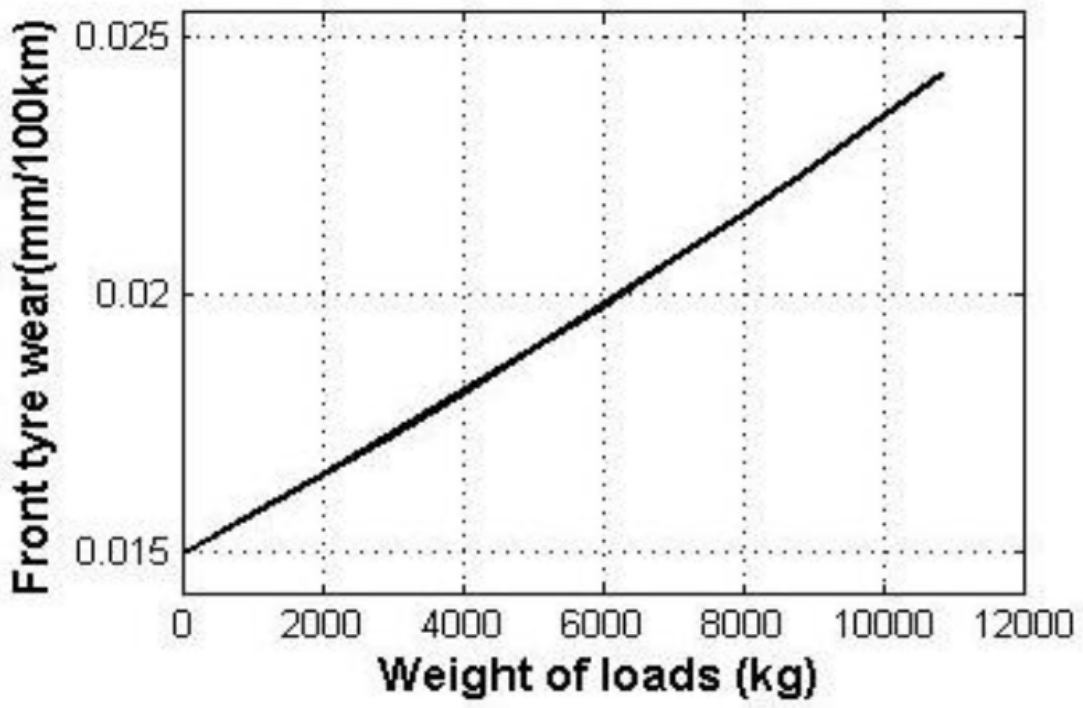

Figure 5.9: Wear as a function of the vertical load, used for validation, [32].

Comparing Figures 5.8 and Figure 5.9 its clear that validation figure measures the load in kg while its measured in N in the thesis. Multiplying the validation data with g = 9.82 N/m^2 will yield the unit N. It can be noticed that the range of the load covered in the Figure 5.8 is represented by a fraction of the representation in the validation figure, Figure 5.9. The behaviour of the validation figure can with good accuracy be approximated as a straight line, in the same range as the span in Figure 5.8. The wear trend of the red curve in Figure 5.8 is of exponentially increasing behaviour as the normal load increases. Comparing the trend in Figure 5.8 and 5.9 it can be seen that the trend is not quite the same. The blue curve in Figure 5.8 is most likely subject to the same numerical error as the forward velocity and the tyre inflation pressure. The red curve, the curve fitting of the model results, is therefore used to compare with the validation results. The difference in trend between the validation results and the curve fitting of the model results is not significant, however should larger loads be considered the difference would be more evident, as the model curve is increasing exponentially. Comparing the values of the two results is difficult since [32] and Figure 5.9 does not indicate the nominal load, the current forward velocity, the side-slip angle or the tyre inflation pressure. However, by comparing the validation results with the results in Figure 5.8 its clear that the gradient of the wear curve in the thesis is larger than the validation curve. A better fitting results could be achieved by alter the Archar's wear equation parameter K. Lower K would yield lower wear which scales linearly, meaning that the trend of the wear would remain the same.

5.6 Wear as a function of forward velocity and side-slip angle

The wear as a function of the forward velocity and side-slip angle is illustrated in Figure 5.10.

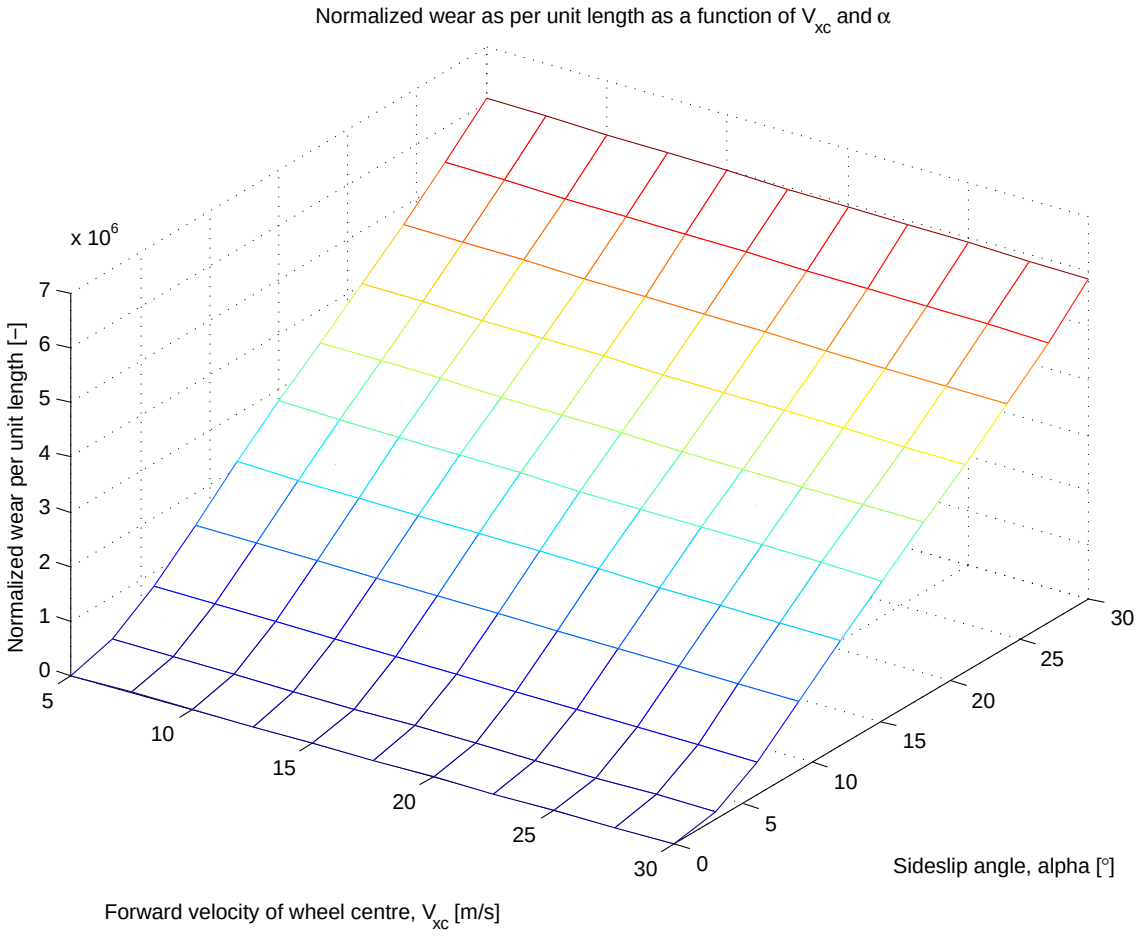

Figure 5.10: Normalized wear as a function of forward velocity and side-slip angle. While the wear is plotted, the rest of the input parameters are fixed at the Q_0 case, meaning $f_{z0} = 9.82 \cdot 350$ N, $M_e = 0$ Nm and $p_t = 1$.

The motivation for plotting Figure 5.10 was to simulate the wear while cornering at a range of forward velocities. Using the results its apparent that side-slip angle plays a much larger role in the wear of tyres compared to the forward velocity. This would suggest that taking a corner with a large radius as possible would minimize the side-slip angle and therefore the wear. Side-slip angle could also arise from other than sources than cornering, such as side wind, these effect are difficult to predict though and are disregarded in the thesis.

5.7 Wear as a function of forward velocity and vertical bristle stiffness

The surface fitting of the normalized wear as a function of forward velocity and bristle stiffness is illustrated in Figure 5.11. The bristle stiffness is related to the tyre inflation pressure as described in Chapter 4 Description of the tyre model. The motivation behind surface fitting the results is that it gives a clearer picture of the wear trend.

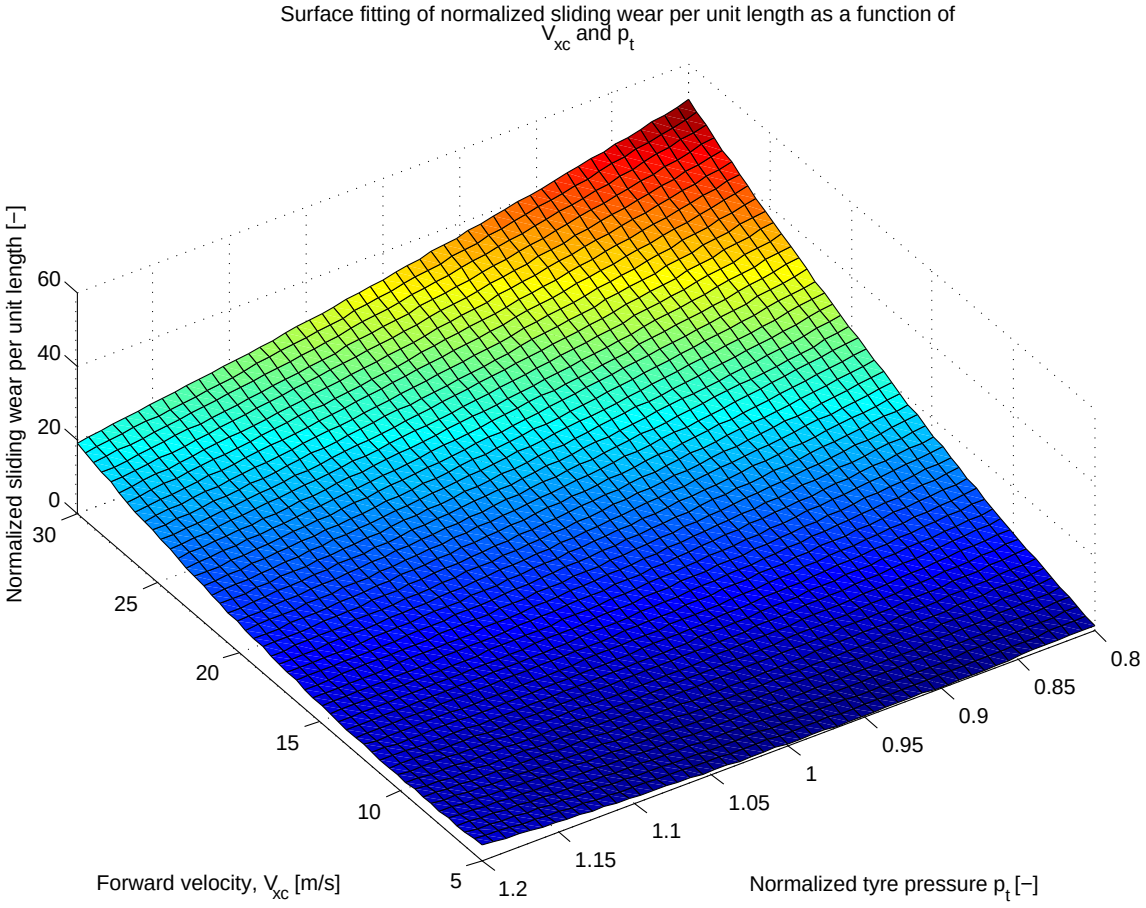

Figure 5.11: Surface fitting of the normalized wear as a function of forward velocity and tyre inflation pressure. For this wear case the rest of the input parameters are fixed at the Q_0 values, meaning $f_{z0} = 9.82 \cdot 350$ N, $M_e = 0$ Nm and $\alpha = 0°$

Figure 5.11 is meant to illustrate the scenario of heating of the tyre for a range of forward velocities. Heating will results in a tyre inflation pressure increase, which is likely to happen during long drives, for example long distance highway driving. The higher the inflation pressure in the tyre the smaller the tyre wear. And as the forward velocity increases the wear also increases. Both these behaviours seem logical and and hence are considered somewhat valid.

5.8 Wear as a function of forward velocity and vertical load

The surface fitting of the normalized wear as a function of forward velocity and vertical load is illustrated in Figure 5.12. The motivation behind surface fitting the results is that it gives a clearer picture of the wear trend.

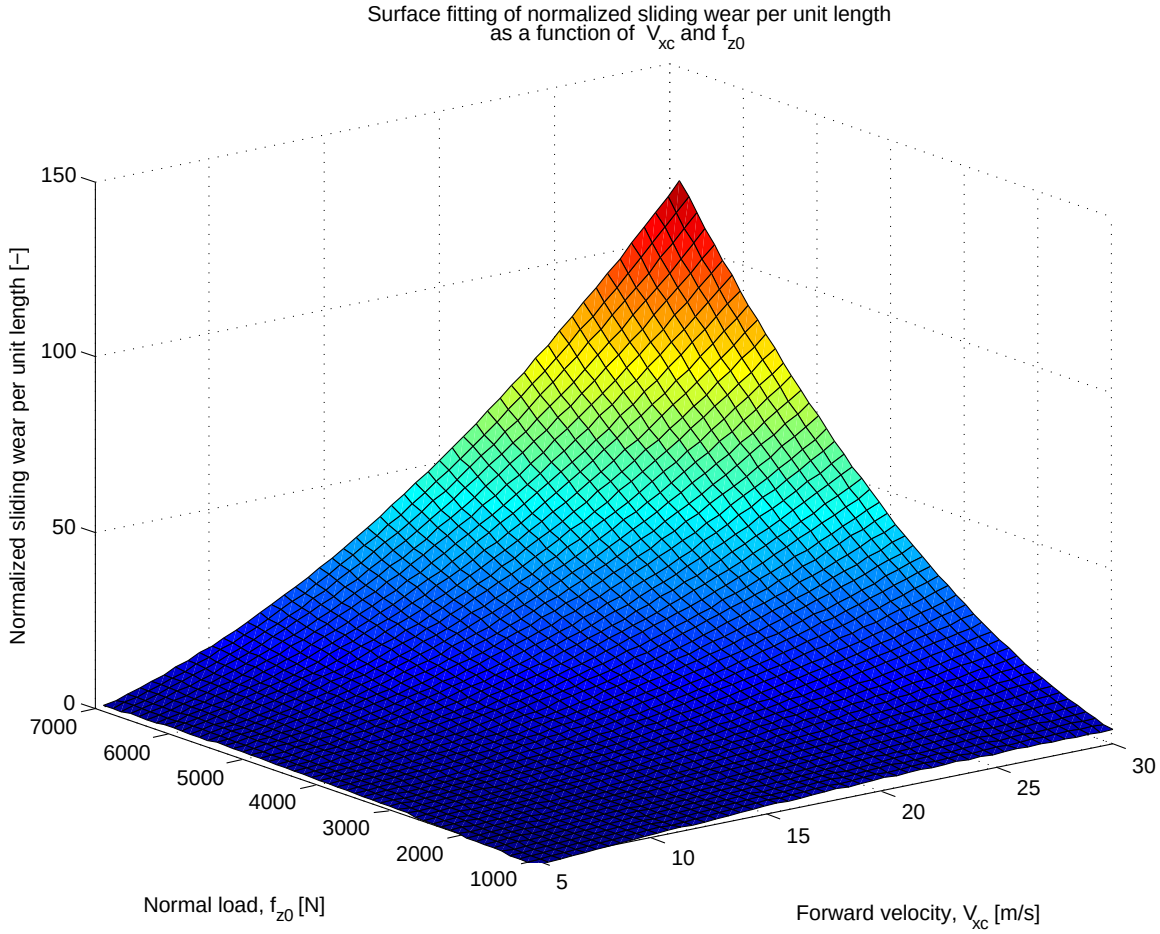

Figure 5.12: Surface fitting of the normalized wear as a function of forward velocity and vertical load. For this wear case the rest of the input parameters are fixed at the Q_0 values, meaning $\alpha = 0°$, $p_t = 1$ and , $M_e = 0$ Nm.

Figure 5.12 is meant to illustrate how the wear behaves while braking or accelerating. While braking or accelerating the center of gravity of the car shifts forward or backward, respectively. The reason why the center of gravity shifts is because of the suspension and the flexibility of the tyres. While braking there is a higher load on the front tyres compared to the back tyres, while accelerating the situation is reversed. From Figure 5.12 it can be seen that the impact of the forward velocity increases with higher vertical loads. This seems reasonable since higher loads lead to greater bristle deflection and higher forward velocities lead to larger longitudinal forces, the result is larger wear for higher loads and higher forward velocities.

Chapter 6

Conclusion and future work

6.1 Conclusion

The objective of the thesis was to gain a better understanding of tyre models and tyre wear and, most importantly, create a user-friendly and trend-accurate wear model of tyres. The model should be able to simulate accurate trends in the conditions; side-slip angle, longitudinal slip, range of forward velocities, change in tyre inflation pressure and change in vertical load.

The tyre wear model show the trend of the wear. The gradient of the curve can be altered to fit the validation data better by adjusting the dimensionless parameter K, from Archard's wear equation.

The wear as a function of the side-slip angle increase exponentially, this trend corresponds with the validation data. The side-slip angle has a very large effect on the wear yielding wear values up 10^6 times higher than the reference case Q_0. The wear as a function of longitudinal slip lacked validation data, the trend of the results show exponentially increasing wear as the longitudinal slip increases, during acceleration or $\lambda \geq 0$. It yields a similar trend for braking or $\lambda \leq 0$, but the wear gradient is not as extreme. The wear as a longitudinal has a very large effect on the wear yielding values of wear up to 10^7 times higher than the reference case Q_0.The wear as a function of tyre inflation pressure decreases linearly as the vertical bristle stiffness increases. The wear as a function of the vertical load increases exponentially as the load increases. The wear as a function of the forward velocity increases exponentially, which corresponds with the validation data.

The surface figures show behaviours which are common occurrences while driving. The conclusion that can be drawn from the results illustrating wear as a function of the forward velocity and side-slip angle is that; taking a corner as widely as possible minimizes wear on the tyres, as it minimizes the side-slip angle. The velocity at which the tyre is travelling has a very small effect on the wear compared to the side-slip angle. The forward velocity and tyre inflation pressure results indicate that during long drives the wear rate will actually decrease, as the tyre heats up and as a results the inflation pressure rises. The conclusion that could be drawn from the forward velocity and vertical load wear case is that high loads impact wear more than low loads and that higher forward velocities affect wear more than lower forward velocities. These results does correlate well with the reality, since higher loads should yield greater tyre deformation and higher velocities yield greater adhesion and cut growth, leading to greater wear. The most severe driving condition occurs during cornering and accelerating or braking. The conclusion that can be drawn from the results are that minimizing longitudinal slip and side-slip angle is of utmost importance in order to reduce wear while driving. The side-slip angle has a larger effect on wear at low longitudinal slip values, the effect diminishes as the longitudinal slip increases but does still generate wear. To conclude, the tyre wear model gives some indication of wear trends but needs to be further developed.

6.2 Future work

Future work on the model include modifications and improvements in order to include more input parameters and possibly take into account the effect of temperature, camber angle or other limitations stated in the report. Another aspect to improve upon is to minimize the oscillations occurring when determining the wear as a function of the forward velocity, tyre inflation pressure and normal load. These trends are the ones furthest from the validation results. Improving the equations governing these results could possible improve the trend of the wear to better fit the validation results. Finding better validation data may have a large impact on the validity of the results, since some of the validation data is gathered from heavy trucks, while the thesis results are oriented towards passenger cars. An alternative to this would be to create a test setup and measure the wear result of each of the input parameters in the thesis. This would perhaps yield the most accurate validation results.

Bibliography

[1] *Worldometers,real time world statistics*, available at: http://www.worldometers.info/cars (Accessed: 17th April 2014)

[2] Foad Mahammadi: *Tire Characteristics Sensitivity Study.* Chalmers University of Technology, Gothenburg, 2012

[3] *Nankang, tyre structure*, available at: http://www.nankang-tyre.com/home.php?fn=eur/wiki (Accessed: 17th April 2014)

[4] *Ctyres, tread design information*, available at: http://www.ctyres.co.uk/tyre_info/tyretread design.html (Accessed: 17th April 2014)

[5] *Tyre wikipedia page*, available at: http://en.wikipedia.org/wiki/Tire (Accessed: 17th April 2014)

[6] *Bridgestone, structure of radial tyre*, available at: http://www.bridgestone.co.in/BasicStructureOfRadial Tyre.aspx (Accessed: 17th April 2014)

[7] *Motera, dictionary of automotive terms*, available at: http://www.motorera.com/dictionary/bi.htm (Accessed: 17th April 2014)

[8] *Tirerack, tyre information*, available at: http://www.tirerack.com/tires/tiretech/techpage.jsp?techid=46 (Accessed: 17th April 2014)

[9] Gäfvert, Magnus and Svendenius, Jacob: *Construcion of Novel Semi-Empirical Tire Models for Combined Braking and Cornering.* Department of Automatic Control Lund Institute of Technology, Lund, April 2003

[10] Toshimichi Takahashi and Masatoshi Hada *Modeling of tire overturning moment characteristics and the analysus of their influence on vehicle rollover behaviour.* Vehicle System Dynamics: International Journal of Vehicle Mechanics and Mobility, Volume 42, issue 1-2, 2004.

[11] *National, tyres and autocare, steering and suspension setup*, available at: http://www.national.co.uk/information/shock-absorbers.aspx (Accessed: 17th April 2014)

[12] *Camber angle definition*, available at: http://en.wikipedia.org/wiki/Camber_angle(Accessed: 17th April 2014)

[13] *Camber angle definition and image*, available at: http://www.bestcoiloverguide.com/coilover-parts/camberplates/(Accessed: 17th April 2014)

[14] *Toe definition*, available at: http://en.wikipedia.org/wiki/Toe_(automotive)(Accessed: 17th April 2014)

[15] *Discount tire direct, toe definition and image*, available at: http://www.discounttiredirect.com/direct /infoAlignment.do (Accessed: 17th April 2014)

[16] *Institute for Dynamic Systems and Control, Ackerman steering definition*, available at: http://www.idsc.ethz.ch/Courses/vehicle_dynamics_and_design/11_0_0_Steering_Theroy.pdf (Accessed: 17th April 2014)

[17] *MotoIQ, understanding KPI and caster*, available at: http://www.motoiq.com/MagazineArticles/ID/1982/PageID/3201/The-Ultimate-Handling-Guide-Part-8-Understanding-Your-Caster-King-Pin-Inclination-and-Scrub.aspx (Accessed: 17th April 2014)

[18] Veen, J: *An analytical approach to dynamic irregular tyre wear*. Eindhoven Univerity of Technology, Eindhoven, 2007

[19] *Question answered regarding hysteresis*, available at: http://answers.yahoo.com/question/index?qid=20090513074958AAmEu6n(Accessed: 17th April 2014)

[20] *Article regarding hysteresis*, available at: http://en.wikipedia.org/wiki/Hysteresis(Accessed: 17th April 2014)

[21] *Taber industries, understanding wear*, available at: http://www.abrasiontesting.com/understanding-wear-abrasion/understanding-wear/(Accessed: 17th April 2014)

[22] *Wheels-inmotion, tyre inflation pressure*, available at: http://www.wheels-inmotion.co.uk/forum/index.php?showtopic=2415 (Accessed: 17th April 2014)

[23] *TYREDAMAGE.COM, tyre wear*, available at: http://www.tyredamage.com/content/view/3/4/ (Accessed: 17th April 2014)

[24] *Delft university, road surface properties*,available at: http://www.citg.tudelft.nl/fileadmin/Faculteit/CiTG/Over_de_faculteit/Afdelingen/Afdeling_Bouw/-_Secties/Sectie_Weg_en_Railbouwkunde/-_Leerstoelen/Leerstoel_Wegbouwkunde/-_Onderwijs/-_College_Dictaten/doc/CT3041_UK_Hoofdstuk_8.pdf, page 233 (Accessed: 17th April 2014)

[25] *Bright hub engineering, roads*, available at: http://www.brighthubengineering.com/concrete-technology/45858-concrete-roads-vs-asphalt-roads/(Accessed: 17th April 2014)

[26] Hans B. Pacejka. *Tyre and Vehicle Dynamics*. page 84-86 Delft University of Technology, The Netherlands

[27] *Hartford university, Archards wear, chapter 6 page 2- 4*, availble at: http://www.ewp.rpi.edu/hartford/ ernesto/F2012/FWM/Notes/ch06.pdf (Accessed: 17th April 2014)

[28] Uil, R.T. *Tyre models for steady-state vehicle handling analysis*. Eindhoven Univerity of Technology, Eindhoven, 2007

[29] P. Flores: *Modeling and simulation of wear in revolute clearance joints in multibody systems*. Mechanism and Machine Theory 44 (2009) 1211–1222. Departamento de Engenharia Mecânica, Universidade do Minho, Campus de Azurém, 4800-058 Guimarães, Portugal

[30] *Wear and Wear mechanism, chapter 6 ,* available at: http://www.ewp.rpi.edu/hartford/ ernesto/F2012/FWM/Notes/ch06.pdf, (Accessed: 17th April 2014)

[31] *Rubber Hardness Chart*, available at: http://mykin.com/rubber-hardness-chart(Accessed 2014-05-15)

[32] Zibo Chen, Sharan Prathaban: *Modeling of Tyre Parameters Influence on Transport Productivity for Heavy Trucks*. Chalmers University of Technology, Gothenburg, Sweden, 2013.

[33] K. A. Grosch and A. Shallamach: *Tyre wear at controlled slip.*The Natural Rubber Producers Research Association, Great Britain, 1961.